R-07-13

Design for rock grouting based on analysis of grout penetration

Verification using Äspö HRL data and parameter analysis

Shinji Kobayashi, Shimizu Corporation/
Kungliga Tekniska Högskolan

Håkan Stille, Kungliga Tekniska Högskolan

January 2007

SKB

Design for rock grouting based on analysis of grout penetration

Verification using Äspö HRL data and parameter analysis

Shinji Kobayashi, Shimizu Corporation/
Kungliga Tekniska Högskolan

Håkan Stille, Kungliga Tekniska Högskolan

January 2007

Preface

This report concerns the ability to predict and design rock fracture grouting. The focus is on the relationship between time and penetration length as developed and presented by Gustafson and Claesson. The theoretical relationship shows that the ratio between actual penetration length and maximum penetration length at a certain time is independent of fracture size. This implies that knowing the dimensions of a fracture system, and having assessed the desired penetration length, the criterion for stopping the grout injection process can be formulated as a time stop criterion. Such theoretically based stop criteria were derived and examined by Gustafson and Stille.

This theoretically based relationship is thus of interest for a well founded grouting design. However, in order to validate the theory, evaluations have to be carried out comparing theory with practical outcome. This report contains such an evaluation, using data collected from the construction of the SKB Äspö TASQ-tunnel "the Apse tunnel" at the Äspö HRL. Furthermore it develops the theory, taking into account the use of different grouts.

Calculations, evaluation and reporting were carried out by Shinji Kobayashi, guest researcher from Shimizu Corporation, Japan, during his stay at the Division of Soil and Rock Mechanics at the Royal Institute of Technology in Stockholm, Sweden. The work was supervised by Professor Håkan Stille and reviewed by PhD Lars Hässler, Golder Associates.

Stockholm, January 2007

Ann Emmelin

Summary

Grouting as a method to reduce the inflow of water into underground facilities will be important in both the construction and operation of the deep repository. SKB has been studying grouting design based on characterization of fractured rock and prediction of grout spread. However, as in other Scandinavian tunnels, stop criteria have been empirically set so that grouting is completed when the grout flow is less than a certain value at maximum pressure or the grout take is above a certain value. Since empirically based stop criteria are determined without a theoretical basis and are not related to grout penetration, the grouting result may be inadequate or uneconomical. In order to permit the choice of adequate and cost-effective grouting methods, stop criteria can be designed based on a theoretical analysis of grout penetration. The relationship between grout penetration and grouting time has been studied at the Royal Institute of Technology (KTH) and Chalmers University of Technology. Based on these studies, the theory has been further developed in order to apply to real grouting work.

Another aspect is using the developed method for parameter analysis. The purpose of parameter analysis is to evaluate the influence of different grouting parameters on the result. Since the grouting strategy is composed of many different components, the selection of a grouting method is complex. Even if the theoretically most suitable grouting method is selected, it is difficult to carry out grouting exactly as planned because grouting parameters such as grout properties can easily vary during the grouting operation. In addition, knowing the parameters precisely beforehand is impossible because there are uncertainties inherent in the rock mass. Therefore, it is important to asses the effects of variations in grouting parameters. The parameter analysis can serve as a guide in choosing an effective grouting method.

The objectives of this report are to:

- Further develop the theory concerning the relationship between grout penetration and grouting time to derive theoretically based stop criteria for real grouting work.

- Verify the theory by using the field data from the grouting experiment at the 450 m level in the Äspö HRL.

- Analyze the difference between the grouting result based on theoretically based stop criteria and that based on empirically based stop criteria.

- Evaluate the effect of variations in grouting parameters such as grouting pressure and grout materials.

The further developed grouting theory includes models for increasing the grouting pressure and changing the grout mix and the capacity of grouting equipment. The theory focuses on deriving theoretically based stop criteria for real grouting work.

The further developed theory was verified by comparing the calculated result with the measured result of the grouting experiment at the 450 m level of the Äspö HRL. It was concluded that the further developed theory is well verified and is applicable to grouting design and analysis, even though there is still room for further improvement.

The difference between the grouting results based on three types of stop criteria – one based on grout flow, one on grout take, and the third on grout penetration – has been analyzed for 1D and 2D flows. Three types of hypothetical rock masses with different permeabilities are used for the calculation. In both the 1D and 2D cases, great differences were found between the results derived from the three stop criteria. In general, grouted volume and grouting time for the 2D case were much higher than those for the 1D case. The results show the importance of choosing the theoretically based stop criteria based on the estimated flow dimension of the fracture system in order to avoid inadequate or uneconomical grouting.

The parameter studies were conducted to show the effect of variation in grouting parameters. As a result of the parameter studies, it was found that the grouting time and the final grouting flow depend on the capacity of the grouting equipment in highly permeable rock, because the capacity of the grouting equipment may be lower than the theoretical grout flow. It was also found in this case that the calculated grouting time is proportional to the grouting pressure and the calculated grouting time is inversely proportional to the viscosity of the grout if the capacity of the grouting equipment is higher than the theoretical grout flow. On the other hand, it was found in this case that the calculated grouting time and the final grout flow are not influenced much by the yield strength of the grout.

Theoretical design based on grout penetration is very useful in choosing a good grouting design. Since the further developed theory takes into account parameters such as increasing the grouting pressure, use of more than one grout and limited equipment capacity, it is widely applicable to analysis of grouting designs and makes it easy to calculate the grouting results.

Sammanfattning

Injektering kommer att användas för att reducera inläckaget till ett kommande underjordiskt förlagt slutförvar. SKB har i olika projekt studerat frågor såsom hur bergets spricksystem ser ut och hur injekteringsbruk sprider sig i bergets sprickor. Svaret på när en injektering skall avbrytas har hittills varit empiriskt grundat. Vanligtvis avbryts injekteringen när flödet understiger ett visst värde för ett givet tryck eller när den injekterade volmen överstiger ett givet värde. Dessa empiriska kriterier har ingen teoretisk grund vilket gör att injekterings-resultatet kan vara både oekonomiskt och otillräckligt.

Forskning utförd vid KTH och Chalmers har dock kunnat visa på teoretiska samband mellan inträngning och flöde. Utgående från dessa teorier har en studie utförts för att belysa hur stoppkriterier för injekteringsarbeten skall väljas för att få en mer optimal injektering.

Dessa teorier har i studien utvecklats ytterligare och applicerats på utförda injekteringar i Apse-tunneln för att validera metodiken. En känslighetsanalys har gjorts för att belysa hur olika parametrar påverkar inträngningen och därmed injekteringsresultatet. Detta har gjorts med tanke på den komplexa process som injekteringen utgör och för att på så sätt ge riktlinjer för vilka faktorer som måste beaktas för att erhålla en effektiv injektering.

Syftet med studien har därför varit att:

• Utveckla de grundläggande teorierna till praktiska verktyg för val av stoppkriterier

• Validera teorierna mot fältdata från injekteringsarbetena för Apse-tunneln (TASQ) i Äspölaboratoriet

• Analysera skillnaden mellan verkliga och teoretiskt beräknade injekteringsresultat

• Utvärdera hur olika faktorer påverkar injekteringsförloppet och resultatet.

Utvecklingen av teorierna har varit inriktad på att kunna beakta ändring av injekteringstryck och injekteringsbruk under själva injekteringsförloppet samt hur utrustningens kapacitet påverkar förloppet.

I samband med byggande av tunneln för Apse-projektet i Äspö på 450 m nivån utfördes ett mindre injekteringsförsök. Detta försök har analyserat med de utvecklade teorierna. En god överensstämmelse erhölls vilket visar att den utvecklade metodiken kan användas för att styra injekteringsförloppet även om det finns rum för förbättringar.

Analysen av skillnaden mellan olika typer av stoppkriterier, (flöde, injekterad volym och inträngning) har studerats för såväl 1-D som 2-D flöde av bruket. Tre olika hypotetiska berg-formationer med olika hydrauliska konduktiviteter har studerats. Analysen visar vikten av att välja stoppkriteriet utifrån teorin och inte på basis av tumregler om man vill undvika oekonomisk eller otillräcklig injektering. Av vikt är att korrekt bestämma dimensionaliteten av bruksflödet.

Utvärderingen av hur olika faktorer påverkar injekteringsförloppet visade att såväl injekterings-tiden som flödet vid stopp beror på kapaciteten på blandningsutrustningen speciellt i permeabelt berg. Injekteringstiden är direkt proportionell mot injekteringstrycket och omvänt proportionellt mot brukets viskositet. I de fall som studerats i rapporten har brukets flytgräns en mindre betydelse på injekteringstiden.

Sammanfattningsvis har studien visat att val av stoppkriterier görs bäst utifrån en teoretisk analys av injekteringsförloppet baserat på den utvecklade teorin som presenterats i rapporten.

Contents

1 Introduction

1.1 Background

Grouting as a method to reduce the inflow of water into underground facilities will be important in both the construction and operation of the deep repository. In two previous PhD projects /Fransson 2001, Eriksson 2002/ and a field experiment at the 450 m level in the Äspö HRL /Emmelin et al. 2004/, SKB has studied grouting design based on characterization of fractured rock and prediction of grout spread. However, as in other Scandinavian tunnels, stop criteria have been empirically set so that grouting is completed when the grout flow is less than a certain value at maximum pressure or the grout take is above a certain value. Since empirically based stop criteria are determined without a theoretical basis and are not related to grout penetration, the grouting result may be inadequate or uneconomical, see Figure 1-1. In order to permit the choice of adequate and cost-effective grouting methods, stop criteria can be designed based on a theoretical analysis of grout penetration.

The relation between grout penetration and grouting time has been studied at the Royal Institute of Technology (KTH) and Chalmers University of Technology. /Hässler 1991/ studied the flow of the grout and formulated the equation in a rectangular channel. /Håkansson 1993/ gave the same equation in a pipe. /Eriksson 2002/ predicted the grout spread and the sealing effect by using a numerical model. The prediction of groutability by calculating the maximum penetration length from grout properties and hydrogeological data was studied in /Gustafson and Stille 1996/. Basic equations of the relationship between relative grout penetration and relative grouting time were derived in /Gustafson and Claesson 2005/, and theoretically based stop criteria for rock grouting were examined in /Gustafson and Stille 2005/. However, a further development of the theories would simplify the implementation in real grouting works.
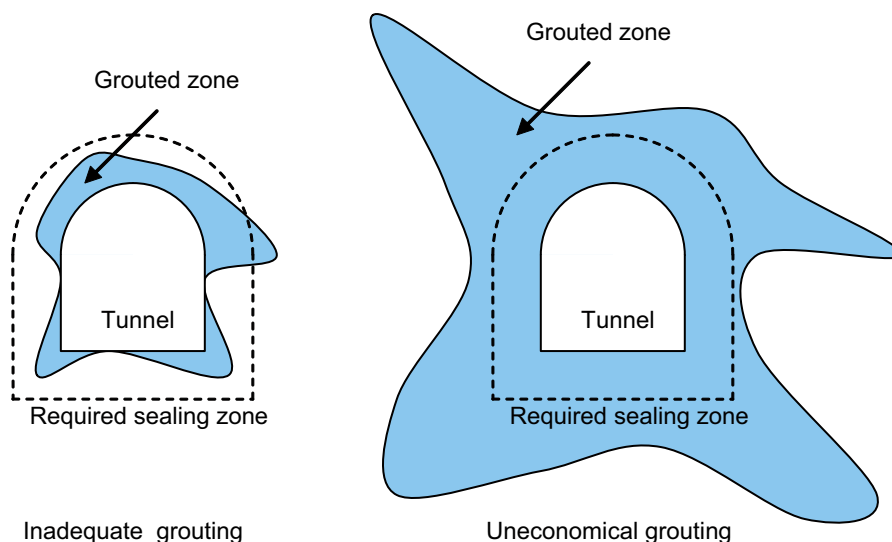
Figure 1-1. *Illustration of inadequate grouting and uneconomical grouting. In the illustration on the left, the grout does not penetrate the required sealing zone. In the illustration on the right, the grout has spread too far.*

Another aspect is using the developed method for parameter analysis. The purpose of parameter analysis is to evaluate the influence of different grouting parameters on the results. Since the grouting strategy is composed of many different components, the selection of a grouting method is complex. Even if the theoretically most suitable grouting method is selected, it is difficult to carry out grouting exactly as planned because grouting parameters such as grout properties can easily vary during the grouting operation. In addition, knowing the parameters precisely beforehand is impossible because there are uncertainties inherent in the rock mass. Therefore, it is important to asses the effect of variation in grouting parameters. The parameter analysis can serve as a guide in choosing an effective grouting method.

1.2   Objectives

The objectives of this report are to:

- Further develop the theory concerning the relationship between grout penetration and grouting time to derive theoretically based stop criteria for real grouting work.

- Verify the theory by using the field data from the grouting experiment at the 450 m level in the Äspö HRL.

- Analyze the difference between the grouting results based on theoretically based stop criteria and those based on the empirically based stop criteria.

- Evaluate the effect of variations in grouting parameters such as grouting pressure and grout materials.

2   Theory of grout penetration

2.1   Overview

The relationship between relative grout penetration and relative grouting time was derived in /Gustafson and Claesson 2005/ and it means that the relative grout penetration, which is defined as the ratio between the actual penetration and the maximum penetration, is the same in all fractures. Based on this study, theoretically based stop criteria for rock grouting were examined in /Gustafson and Stille 2005/. These are based on a single Bingham fluid model in parallel planar fractures with constant aperture at constant grouting pressure. However, grouting is more complicated in reality. A further development of the theories would simplify the implementation in real grouting works. The further developed theory includes increasing the grouting pressure and changing the grout mix and the capacity of the grouting equipment such as grout pump and grout mixer.

2.2   Grout penetration of a Bingham fluid at constant pressure

2.2.1   Basic equations

The relationship between grout penetration and grouting time is obtained from two basic equations. One is based on a simple force balance when grouting is completed and the other is obtained from the Navier-Stokes equation.

Cement grouts can be described as Bingham fluids characterized by a yield strength τ_0 and a plastic viscosity μ_g. According to /Gustafson and Stille 1996/, the maximum penetration at steady state into a fracture aperture b can be calculated as:

$$I_{max} = \left(\frac{\Delta p}{2\tau_0}\right) \cdot b \qquad\qquad (2\text{-}1)$$

where $\Delta p = p_g - p_w$ is the grouting pressure, see Figure 2-1.
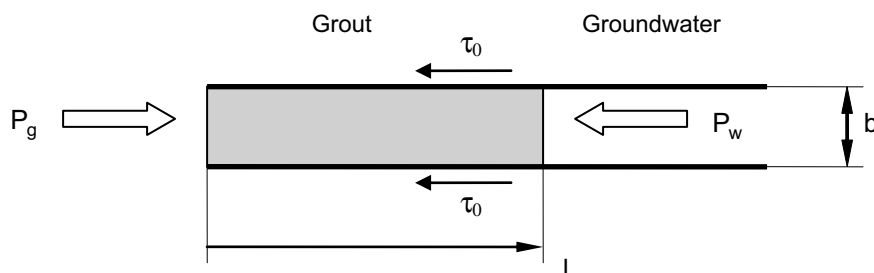
Figure 2-1. *Grout penetration of a Bingham fluid. P_g is the injection pressure produced by the grout pump and P_w is the groundwater pressure.*

From the Navier-Stokes equation, the flow (or velocity) of grout, dI/dt, can be calculated according to /Hässler 1991/ as:

$$\frac{dI}{dt} = -\frac{dp}{dx} \cdot \frac{b^2}{12\mu_g}\left[1 - 3\cdot\frac{Z}{b} + 4\cdot\left(\frac{Z}{b}\right)^3\right]$$

(2-2)

where

$$Z = \tau_0 \cdot \left|\frac{dp}{dx}\right|^{-1}, \quad Z < \frac{b}{2}$$

(2-3)

2.2.2 Approximations for analytical grout penetration

In order to obtain analytical solutions for grout penetration, the characteristic grouting time t_0, the relative grouting time t_D, and the relative grouting penetration I_D are defined according to /Gustafson and Stille 2005/ as:

$$t_0 = \frac{6\Delta p \cdot \mu_g}{\tau_0^2}$$

(2-4)

$$t_D = \frac{t}{t_0}$$

(2-5)

$$I_D = \frac{I}{I_{max}}$$

(2-6)

Using the equations (2-1) to (2-6), approximations of the relationships between the relative penetration and the relative time for both the one-dimensional (1D) and the two-dimensional (2D) cases are derived by /Gustafson and Stille 2005/ as:

$$I_D = \sqrt{\theta^2 + 4\theta} - \theta$$

(2-7)

$$\theta_{1D} = \frac{t_D}{2(0.6 + t_D)}$$

(2-8)

$$\theta_{2D} = \frac{t_D}{2(3 + t_D)}$$

(2-9)

The plots of I_D as a function of t_D are shown in Figure 2-2.
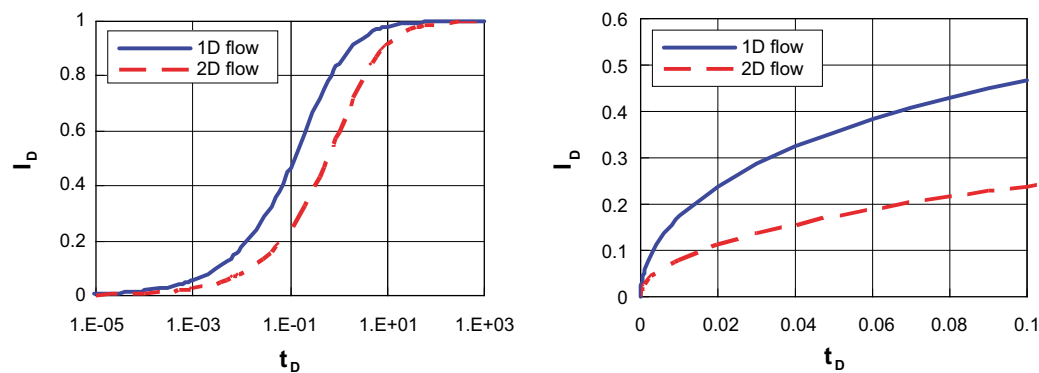
Figure 2-2. *Approximations of relative penetration as a function of relative time for 1D and 2D cases. In the graph on the left the X axis is logarithmic. In the graph on the right X axis has a normal scale.*

14

2.2.3 Grout volume and flow

For the 1D case, the volume injected into the channel at width w and aperture b is calculated as:

$$V = I \cdot w \cdot b = I_D \cdot I_{max} \cdot w \cdot b = I_D \cdot \left(\frac{\Delta p}{2\tau_0}\right) \cdot w \cdot b^2 \qquad (2\text{-}10)$$

This is calculated for several fractures as:

$$V_{tot} = I_D \cdot \left(\frac{\Delta p}{2\tau_0}\right) \cdot \sum wb^2 \qquad (2\text{-}11)$$

The grout flow can be calculated as:

$$Q = \frac{dV_{tot}}{dt} = \frac{dI_D}{dt_D} \cdot \frac{1}{t_0} \cdot \left(\frac{\Delta p}{2\tau_0}\right) \cdot \sum wb^2 \qquad (2\text{-}12)$$

For the 2D case, the volume injected into the circular fracture with aperture b is calculated as:

$$V = \pi \cdot I^2 \cdot b = \pi \cdot \left(I_D \cdot I_{max}\right)^2 \cdot b = \pi \cdot I_D^2 \cdot \left(\frac{\Delta p}{2\tau_0}\right)^2 \cdot b^3 \qquad (2\text{-}13)$$

This is calculated for several fractures as:

$$V_{tot} = \pi \cdot I_D^2 \cdot \left(\frac{\Delta p}{2\tau_0}\right)^2 \cdot \sum b^3 \qquad (2\text{-}14)$$

The grout flow can be calculated as:

$$Q = \frac{dV_{tot}}{dt} = 2\pi \cdot I_D \cdot \frac{dI_D}{dt_D} \cdot \frac{1}{t_0} \cdot \left(\frac{\Delta p}{2\tau_0}\right)^2 \cdot \sum b^3 \qquad (2\text{-}15)$$

2.3 Further development of the theory

2.3.1 Increasing grouting pressure

Since grouting normally starts at a low grouting pressure after which the pressure is increased to the maximum, it is important to include increasing grouting pressure in the theory. The simple case is described that the grouting pressure increases from P_a to P_b at time t_1, see Figure 2-3. In this case, the relationship between time and penetration can be calculated as:

$$I = I_{Pa}(t), \qquad\qquad t < t_1 \qquad (2\text{-}16)$$

$$I = I_{Pb}(t - (t_1 - t_{b1})), \qquad t > t_1 \qquad (2\text{-}17)$$

$$I_{Pb}(t_{b1}) = I_{Pa}(t_1) = I_1 \qquad (2\text{-}18)$$

where $I_{Pa}(t)$ is the relationship between time and penetration under the constant pressure P_a and $I_{Pb}(t)$ is the relationship between time and penetration under the constant pressure P_b.
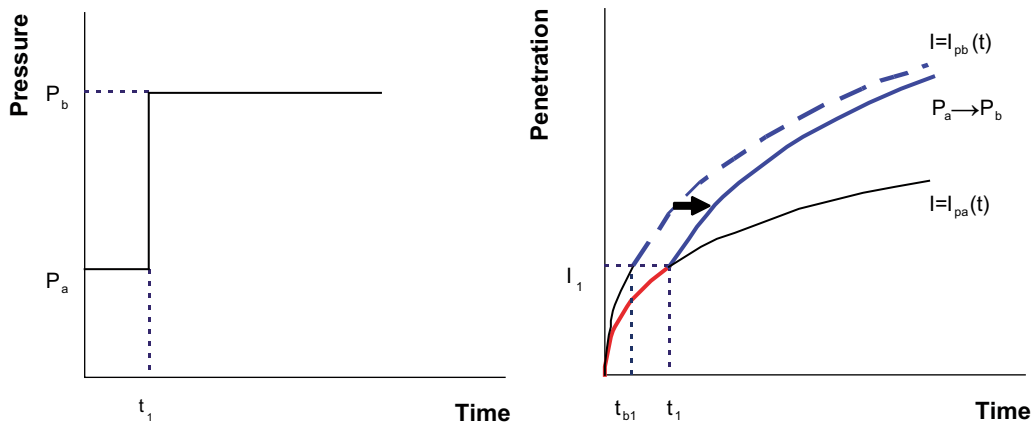
Figure 2-3. *Relationship between time and penetration when the grouting pressure increases from P_a to P_b. The graph on the left shows the relationship between time and grouting pressure. The graph on the right shows how penetration changes as the grouting pressure increases.*

2.3.2 Changing grout mixes

The second development is extending the theory to include changed grout mixes. In normal grouting work, it is quite common to change the recipe from thin grout to thick grout during grouting. The problem is that obtaining the theoretical solution for changing grout mixes is not straightforward. Some manipulations are necessary in order to obtain the approximation. However, the lower and upper boundaries for penetration length after the grout mix is changed from thin grout (Grout A) to thick grout (Grout B) can be solved. In the following calculations, t_1 is used as the time when the grout mix is changed and I_1 is the penetration length.

The lower boundary is calculated on the assumption that the properties of the pre-injected grout (Grout A) are same as those of new grout (Grout B). On this assumption, grout penetration after time t_1 can be described by using the penetration curve for new grout (Grout B) from penetration I_1 as:

$$I = I_{Ga}(t), \qquad t < t_1 \tag{2-19}$$

$$I = I_{Gb}(t + t_{b1} - t_1), \qquad t > t_1 \tag{2-20}$$

$$I_{Gb}(t_{b1}) = I_{Ga}(t_1) = I_1 \tag{2-21}$$

where $I_{Ga}(t)$ is the relationship between time and penetration of Grout A and $I_{Gb}(t)$ is the relationship between time and penetration of Grout B.

The upper boundary is calculated on the assumption that the properties of the pre-injected grout (Grout A) are the same as those of the groundwater. On this assumption, grout penetration after time t_1 can be described by using the penetration curve for new grout (Grout B) from penetration 0 as:

$$I = I_{Ga}(t), \qquad t < t_1 \tag{2-22}$$

$$I = I_{Ga}(t_1) + I_{Gb}(t - t_1), \qquad t > t_1 \tag{2-23}$$

Figure 2-4 shows how penetration changes after the grout mix is changed.
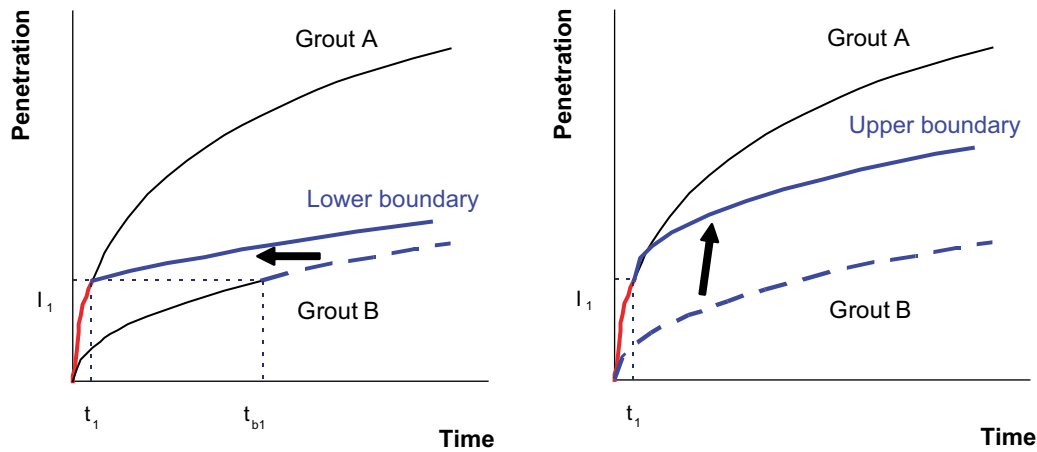
Figure 2-4. *Lower and upper boundaries of relationship between time and penetration when the grout mix changes from Grout A to Grout B. The graph on the left shows the lower boundary and the graph on the right shows the upper boundary.*

2.3.3   Capacity of grouting equipment

The third development is to take the capacity of the grouting equipment into account, such as the grout pump and the grout mixer. In reality the pump may produce lower flow at higher pressure and vice versa. It can be said that the pumping flow is inversely proportional to the pumping pressure, but the pump capacity is restricted to a certain maximum flow and pressure. The capacity of the type of piston pump that is normally used can be described as:

$$P \cdot Q \leq C_p \tag{2-24}$$

$$P \leq P_{p\,\mathrm{max}} \tag{2-25}$$

$$Q \leq Q_{p\,\mathrm{max}} \tag{2-26}$$

where P is pressure, Q is flow, C_p is the pump capacity, P_{pmax} is the maximum pump pressure and Q_{pmax} is the maximum pump flow.

In real grouting work, mixer capacity is also restricted to a certain maximum flow and can be described as:

$$Q \leq Q_{m\,\mathrm{max}} \tag{2-27}$$

where Q_{mmax} is the maximum mixer capacity

Since the maximum pump flow is much higher than the maximum mixer capacity in general, as a practical aspect, the capacity of the grouting equipment for the purpose of the calculation is described by the equations (2-25) and (2-27) as:

$$P \leq P_{p\,\mathrm{max}} \text{ and } Q \leq Q_{m\,\mathrm{max}} \tag{2-28}$$

These capacities are illustrated in Figure 2-5.

Figure 2-5. *Capacities of grouting pump and grouting mixer. The hatched area shows the capacity of the grouting equipment for the purpose of the calculation.*

3 Verification using Äspö HRL data

3.1 Field experiment at Äspö HRL

3.1.1 Overview

The field data from the grouting experiments at Äspö HRL was used in order to verify the further developed theory. A grouting field experiment was carried out at the 450 m level in the Äspö HRL and reported in /Emmelin et al. 2004/. The main objectives of the experiment were to:
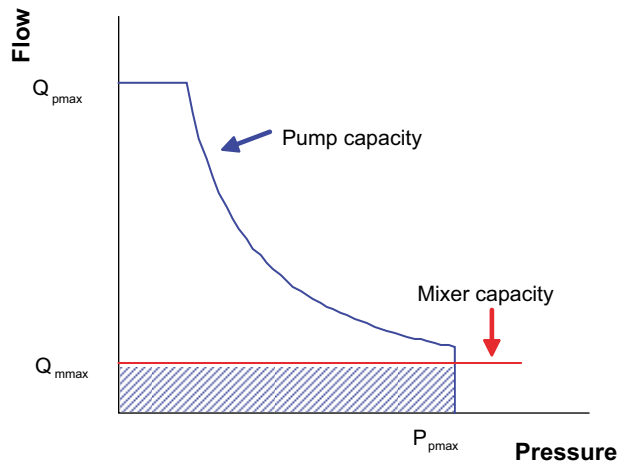
- Investigate what can be achieved with best available technology, material and knowledge under the current conditions, i.e. a relatively tight crystalline rock mass at great depth.

- Collect data and evaluate theories resulting from previous research projects on characterization and predictions of grout spread.

- Collect data to further develop those theories.

- Contribute to the achievement of good conditions at the experimental site for the pillar stability experiments.

In the experiment, the specific capacity (Q/dh) was assumed to provide a description of the conductive fracture where the median specific capacity would be approximately equal to the transmissivity and the variation in specific capacity would provide a picture of variations in aperture within a conductive feature /Fransson 2001/. Based on the description of the fracture, results and choice of grouting design were predicted using a numerical model /Eriksson 2002/. It was found that the predicted grouting volumes were considerably smaller than the obtained volumes and the predicted grouting times deviated from the obtained times, but the sealing effect of the grouting was predicted accurately.

3.1.2 Hydrogeological characterization

Hydraulic apertures used for numerical calculation were estimated based on the specific capacity (Q/dh), which was defined by the inflow during drilling, Q and the hydraulic head measured during a pressure build-up test, dh. It was assumed that the median specific capacity would be approximately equal to the transmissivity and the variation in specific capacity would provide a picture of variations in aperture within a conductive feature. Transmissivity T was calculated using the cubic law as:

$$\frac{Q}{dh} \approx T = \frac{\rho_w g b^3}{12 \mu_w} \tag{3-1}$$

where ρ_w is the density of water, μ_w is the viscosity of water, g is the acceleration due to gravity, and b is the hydraulic aperture of the fracture.

The inflow data and the estimated hydraulic apertures are shown in Appendix A.

The geometrical properties of fractures were interpreted based on the hydraulic apertures using equation (3-2) from /Zimmerman and Bodvardsson 1996/.

$$b^3 = \left(b_{average}^3 \right) \left[1 - \frac{1.5 \sigma_b^2}{b_{average}^2} \right] (1 - 2c) \tag{3-2}$$

where b is the hydraulic aperture, $b_{average}$ is the arithmetic mean aperture, σ_b is the standard deviation in aperture and c is the fraction of the contact area.

In addition to the measurement of natural inflows, water loss measurements were performed only in Fan 1:1 in the experiment (see Appendix B). However, the data was not used for the calculation because it was collected for later evaluation.

3.1.3 Calculation model in previous field experiment

The calculation in the previous field experiment was carried out based on the numerical model presented in /Eriksson 2002/. In the calculation procedure, inflow before and after grouting were calculated according to the flow chart in Figure 3-1. The capacity of the pump and the varying grouting pressure were not taken into account by the model. An example of the calculation result is shown in Figure 3-2.

3.1.4 Grouting design in the previous field experiment

In the previous field experiment the grouting design was modified according to the modified descriptions of the rock mass. Based on the final third description, the experiment was executed in two grouting fans. The first fan (Fan 1) was grouted using two grouting rounds but the second fan (Fan 2) included only one grouting round. The first grouting round of Fan 1 (Fan 1:1) was to be carried out as follows:

- 11 boreholes, 16 m long.
- Minimum flow 1.0 litre/min.
- Grouting pressure 1 MPa above groundwater pressure.
- Borehole radius 0.032 m.
- Grouting starts with Grout B and continues until 150 litres is grouted, if refusal based on the flow criterion is not obtained. After this, change to Grout C and no more than 50 additional litres are grouted. After this grouting is stopped.
- Grouting is carried out in descending order based on specific capacity.

The second grouting round of Fan 1 (Fan 1:2) was to be carried out as follows:

- 20 boreholes, 16 m long.
- Minimum flow 1.0 litre/min.
- Grouting pressure 2 MPa above groundwater pressure.
- Borehole radius 0.032 m.
- Grouting starts with Grout A and continues until 100 litres is grouted, if refusal based on the flow criterion is not obtained. After this, change to Grout B and no more than 50 additional litres are grouted. After this grouting is stopped.
- Grouting is carried out in descending order based on specific capacity.

Fan 2 was to be carried out as follows:

- 21 boreholes, 16 m long.
- Minimum flow 0.2 litre/min.
- Grouting pressure 2 MPa above groundwater pressure.
- Maximum hole distance 2 m.
- Borehole radius 0.032 m.
- Grouting starts with Grout A and, after ~100 litres, the grout is changed to Grout B. Again, after ~50 litres grouting is continued with Grout C. After grouting ~50 litres with this grout, grouting is stopped.

The properties of the two grouts, Grout A and Grout B, were measured both in the laboratory and on site, but the properties of Grout C were not determined since it was only to be used as the final stop grout. The grout properties are listed in Table 3-1.
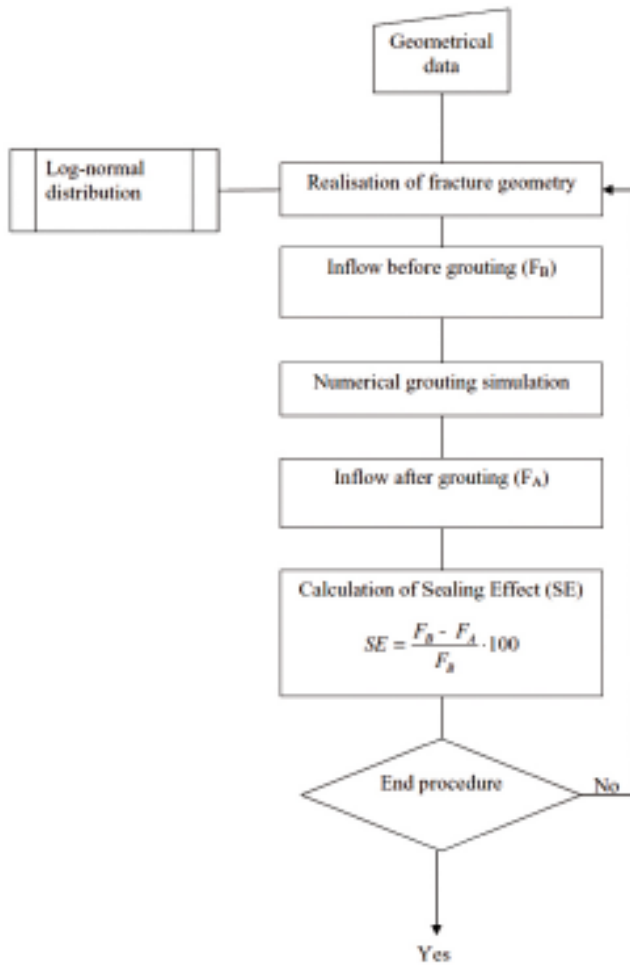
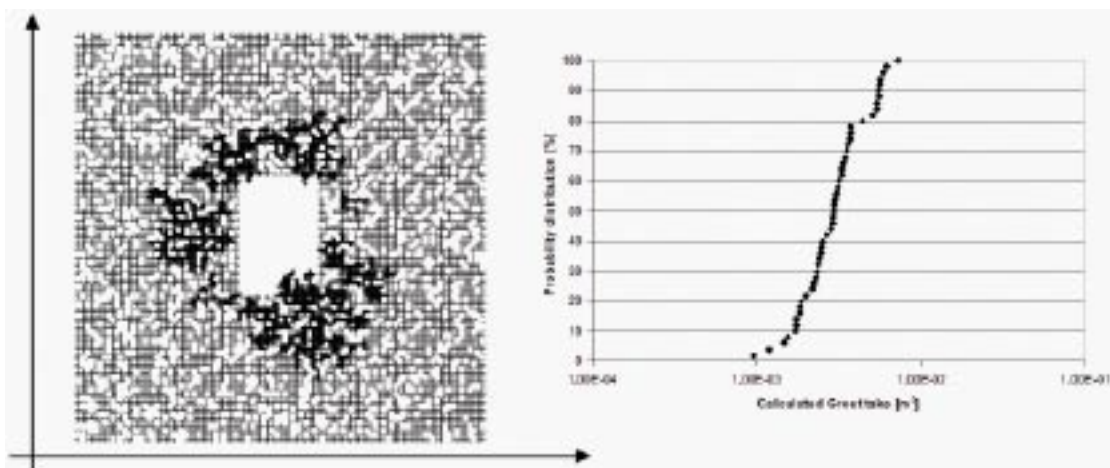**Figure 3-1.** *Illustration of the calculation procedure /Emmelin et al. 2004/.*

Figure 3-2. *An example of the result of a calculation. The left figure shows a realization of a fracture grouting. The right diagram shows the distribution of calculated grout take based on a number of realizations of input data /Emmelin et al. 2004/.*

Table 3-1. Grout properties valid for t<3,600 sec.

Property		Grout		
		A **UF 16, w/c 2.0** **0.9% HPM**	**B** **UF 16, w/c 1.0** **0.9% HPM**	**C** **UF 16, w/c 0.8** **0.9% HPM**
Rheology	Yield value [Pa]	$0.296 \cdot e^{0.0004t}$	$1.5 \cdot e^{0.0004t}$	–
	Viscosity [Pas]	$0.0056 \cdot e^{0.0004t}$	$0.017 \cdot e^{0.0004t}$	–
Penetrability	b_{min} [µm]	37	41	–
	$b_{critical}$ [µm]	$0.0032t+60$	$0.0032t+75$	–
Density	[kg/m^3]	1,290	1,480	–
Bleed	[%]	15	5	–

3.1.5 Predicted grouting results in the previous field experiment

In the previous field experiment the prediction of the grouting results was modified twice with the modified descriptions of the rock mass. The predicted grouting results in the previous field experiment shown below are based on the third and final description.

The predicted grouting results for Fan 1:1 were:

- Total grouted volume excluding filling of the holes   221 litres.
- Grouting time excluding filling of the holes   641 min.
- Sealing effect   97%.

The predicted grouting results for Fan 1:2 were:

- Total grouted volume excluding filling of the holes   46 litres.
- Grouting time excluding filling of the holes   430 min.
- Sealing effect   92%.

The predicted grouting results for Fan 2 were:

- Total grouted volume excluding filling of the holes   291 litres.
- Grouting time excluding filling of the holes   898 min.
- Sealing effect   95%.

3.1.6 Measured grouting results in previous field experiment

Measured grout take and grouting time and evaluated sealing effect in the previous field experiment are shown in Table 3-2. These measured values are presented in detail in Appendix C.

It was found that the predicted grouting volumes were considerably smaller than the obtained volumes and the predicted grouting times deviated from the obtained times, but the sealing effect of the grouting was predicted accurately.

It should be noted that the practical grouting work for Fan 1:1 was not based on the grouting design shown in 3.1.4. According to the measured grouting data, it would appear that the grouting design for Fan 1:1 was changed during operation as follows:

- The grouting starts with Grout B and continues until **100** litres is grouted, if refusal based on the flow criterion is not obtained. After this, change to Grout C and no more than **100** additional litres are grouted. After this the grouting is stopped.

Table 3-2. Summary of measured and evaluated grouting results.

Fan	Grout take [l]	Grouting time [min]	Sealing effect [%]
	Including hole filling/ excluding hole filing	Including hole filling/ excluding hole filing	
1:1	1633/863	196/160	97
1:2	2537/1137	854/800	97
2	2456/1470	480/420	95

3.2 Prediction of grouting result using the further developed theory

3.2.1 Hydraulic apertures

Hydraulic apertures based on inflow during drilling of the grouting holes are used directly for calculation to verify the further developed theory.

In addition to measurement of natural inflows, water loss measurements were performed only in Fan 1:1 in the previous experiment. Transmissivity can be calculated from water loss according to /Gustafson and Stille 1996/ as:

$$T = \frac{Q\rho_w g}{2\pi(P_t - P_w)}\ln\frac{L}{r_w}$$ (3-3)

where Q and P_t are the injection flow and pressure, ρ_w is the density of water, g is the acceleration due to gravity, P_w is the groundwater pressure, L is the length of the test section, and r_w is the radius of the borehole. The number of fractures along each borehole and the aperture ratio between fractures within each borehole are set equal to the values estimated in the previous experiment. The estimated hydraulic apertures based on water loss measurement are listed in Appendix D. These values are significantly greater than those based on inflow (see Figure 3-3). Additional calculation using hydraulic apertures based on water loss measurements is carried out for Fan 1:1.
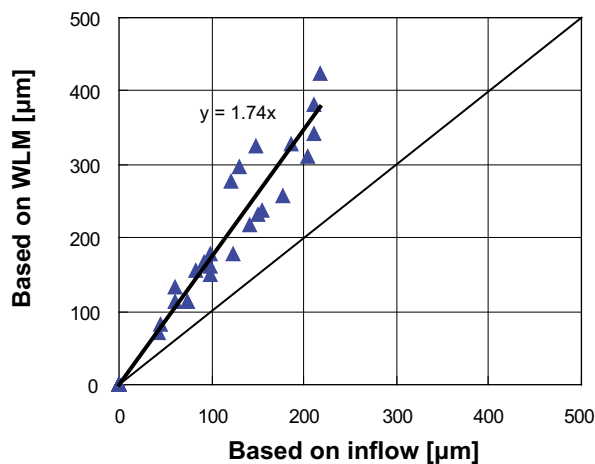

Figure 3-3. *Relationship between hydraulic apertures based on inflow and those based on water loss measurement (WLM) in Fan 1:1.*

3.2.2 Grouting design

The grouting design for calculations to predict the grouting results is used precisely as described in 3.1.4. As noted in 3.1.6, it would appear that the grouting design for Fan 1:1 was changed during operation. An additional calculation for Fan 1:1 is carried out using the changed grouting design.

3.2.3 Grout properties

The grout is characterized in terms of rheology and penetrability. From a temporal point of view, there are two methods for using the properties for the calculation. One is that the properties are described as time-dependent, which was used in the experiment at the Äspö HRL, (see Table 3-1). The other is to use constant properties, which is shown in, for example, /Dalmalm 2004/. In order to avoid complex calculation, the properties at time 0 are used constantly for this prediction.

In the experiment at the Äspö HRL, the grout was characterized with a minimum aperture (b_{min}) and a critical aperture ($b_{critical}$) to include filtration in the model. Critical aperture was defined as the aperture size below which filtration occurs and was denoted ($b_{critical}$), while minimum size was defined as the aperture size below which no grout can pass and was denoted (b_{min}). On the other hand, in this prediction each fracture along boreholes is assumed to be constant and filtration is excluded in the model. Therefore, the minimum groutable aperture ($b_{groutable}$), which is defined in the model as the aperture size below which no grout can pass, is set equal to the minimum aperture (b_{min}) obtained in the previous experiment.

Since the properties of Grout C had not been determined in the experiment at the Äspö HRL, the grout data from /Dalmalm 2004/ is used. The grout properties used for the calculation are shown in Table 3-3.

3.2.4 Calculation

Calculations to predict the grouting results are carried out precisely according to the grouting design described in 3.1.3. In the calculation procedure, each calculation is performed hole by hole for holes which have some fractures with constant aperture.

According to /Emmelin et al. 2004/, fractures are assumed to be planes which are perpendicular to the tunnel and intersect with boreholes. Therefore, the calculation is done for 2D flow.

Figure 3-4 shows an example of the result of a calculation for Fan 1:1. In this case, grouting starts with Grout B and continues until 150 litres is grouted (including hole filling). Since refusal based on the grout flow criterion is not obtained, grouting changes to Grout C. Grouting is completed when the grout flow is less than 1.0 litre/min.

Table 3-3. Grout properties used for the calculation.

Property		Grout		
		A UF 16, w/c 2.0 0.9% HPM	B UF 16, w/c 1.0 0.9% HPM	C UF 16, w/c 0.8 0.9% HPM
Rheology	Yield value [Pa]	0.296	1.5	10.3
	Viscosity [Pas]	0.0056	0.017	0.093
Minimum groutable aperture	$b_{groutable}$ [µm]	37	41	44

Figure 3-4. *An example of a calculation for Fan 1:1. The graph on the left shows the grout flow and the grouting time (excluding hole filling) calculated for the first grout (Grout B). The graph on right shows the same values calculated for the second grout (Grout C).*

3.3　Comparison of calculated and measured results

3.3.1　Results from hydraulic apertures based on inflow

In the first grouting round of Fan 1 (Fan 1:1) the calculated grouting results from hydraulic apertures based on inflow are:

* Lower boundary of total grouted volume excluding filling of the holes　　692 litres.
* Upper boundary of total grouted volume excluding filling of the holes　　692 litres.
* Lower boundary of grouting time excluding filling of the holes　　376 min.
* Upper boundary of grouting time excluding filling of the holes　　376 min.

The upper and lower boundaries of the calculated results for Fan 1:1 are the same because the grouted volumes of the second grout (Grout C) are zero for both cases. The second grout (Grout C) is too thick to be injected into the fractures in Fan 1:1. Figure 3-5 shows a comparison between the calculated and measured results for Fan 1:1. As a reference, the predicted results in the experiment /Emmelin et al. 2004/ noted in 3.1.5 are shown on the right in both figures. The calculated results for every grouting hole in Fan 1:1 are shown in Appendix E.

The calculated grouted volume is close to the measured volume, but the calculated grouting time is greater than the measured value. Compared to the predicted results in the experiment, both grouted volume and grouting time are close to those predicted.

In the second grouting round of Fan 1 (Fan 1:2), the calculated grouting results from hydraulic apertures based on inflow are:

* Lower boundary of total grouted volume excluding filling of the holes　　233 litres.
* Upper boundary of total grouted volume excluding filling of the holes　　263 litres.
* Lower boundary of grouting time excluding filling of the holes　　175 min.
* Upper boundary of grouting time excluding filling of the holes　　203 min.

The difference between the lower and the upper boundaries is small. Figure 3-6 shows a comparison between calculated and measured results for Fan 1:2. The calculated results for every grouting hole in Fan 1:2 are shown in Appendix E.

It is found that both calculated grouted volume and grouting time are much smaller than the measured values.
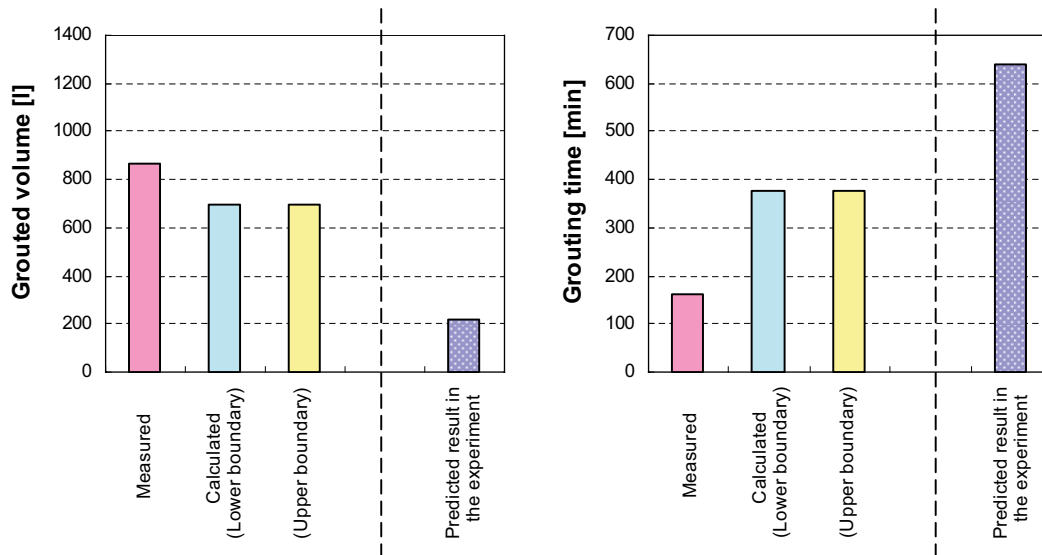
Figure 3-5. *Comparison of calculated results from hydraulic apertures based on inflow and measured results for Fan 1:1. The graph on the left shows grouted volume while the graph on the right shows grouting time. The predicted results in the experiment /Emmelin et al. 2004/ are shown on the right in both figures.*
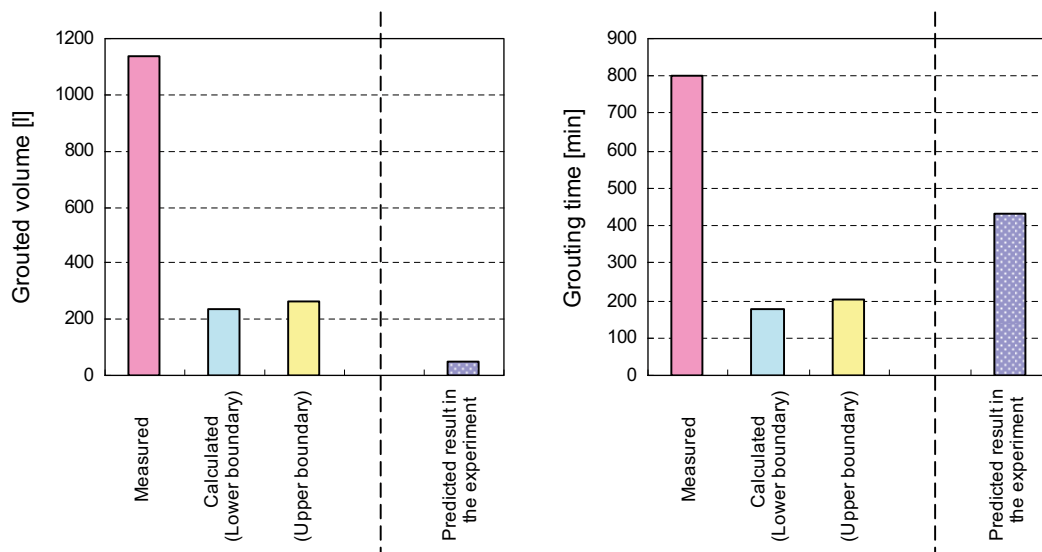

Figure 3-6. *Comparison of calculated results from hydraulic apertures based on inflow and measured results for Fan 1:2. The graph on the left shows grouted volume, while the graph on the right shows grouting time. The predicted results in the experiment /Emmelin et al. 2004/ are shown on the right in both figures.*

In Fan 2, the calculated grouting results from hydraulic apertures based on inflow are:

- Lower boundary of total grouted volume excluding filling of the holes   1,170 litres.
- Upper boundary of total grouted volume excluding filling of the holes   1,219 litres.
- Lower boundary of grouting time excluding filling of the holes   1,632 min.
- Upper boundary of grouting time excluding filling of the holes   1,767 min.

The difference between the upper and the lower boundaries is small. Figure 3-7 shows a comparison between calculated and measured result for Fan 2. The calculated results for every grouting hole in Fan 2 are shown in Appendix E.
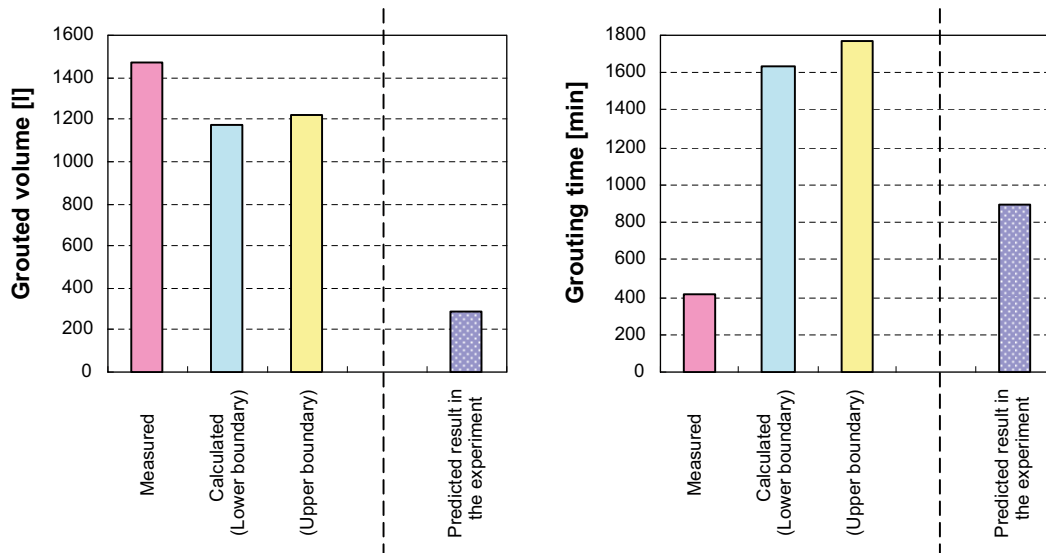
Figure 3-7. *Comparison of calculated results from hydraulic apertures based on inflow and measured results for Fan 2. The graph on the left shows grouted volume, while the graph on the right shows grouting time. The predicted results in the experiment /Emmelin et al. 2004/ are shown on the right in both figures.*

The calculated grouted volume is smaller than the measured volume, whereas the calculated grouting time is significantly greater than the measured value.

3.3.2   Results from hydraulic apertures based on water loss measurement

Water loss measurements were performed only in Fan 1:1 in the experiment. In Fan 1:1 the calculated grouting results from hydraulic apertures based on water loss measurement are:

- Lower boundary of total grouted volume excluding filling of the holes   1,023 litres.
- Upper boundary of total grouted volume excluding filling of the holes   1,238 litres.
- Lower boundary of grouting time excluding filling of the holes   229 min.
- Upper boundary of grouting time excluding filling of the holes   334 min.

Figure 3-8 shows a comparison between calculated results from hydraulic apertures based on water loss measurement and measured results for Fan 1:1. Figure 3-9 shows a comparison between calculated results from hydraulic apertures based on inflow and calculated results from hydraulic apertures based on water loss measurement. The calculated results for every grouting hole are shown in Appendix F.

The calculated grouted volume based on water loss measurement increases is comparable to that based on inflow, whereas the calculated grouting time decreases and approaches the measured value.

Water loss measurements were not performed in Fan 1:2 and Fan 2 in the experiment. However, it is interesting to compare the calculated result based on inflow with the result based on water loss measurement as shown in Figure 3-9. Therefore, for Fan 1:2 and Fan 2, the hydraulic apertures based on water loss measurement are supposed to be estimated according to the relationship between hydraulic apertures based on inflow and those based on water loss measurement for Fan 1:1. The relationship between hydraulic apertures based on inflow, b_{inf}, and those based on water loss measurement, b_{wlm}, for Fan 1:1 can be described according to Figure 3-3 as:
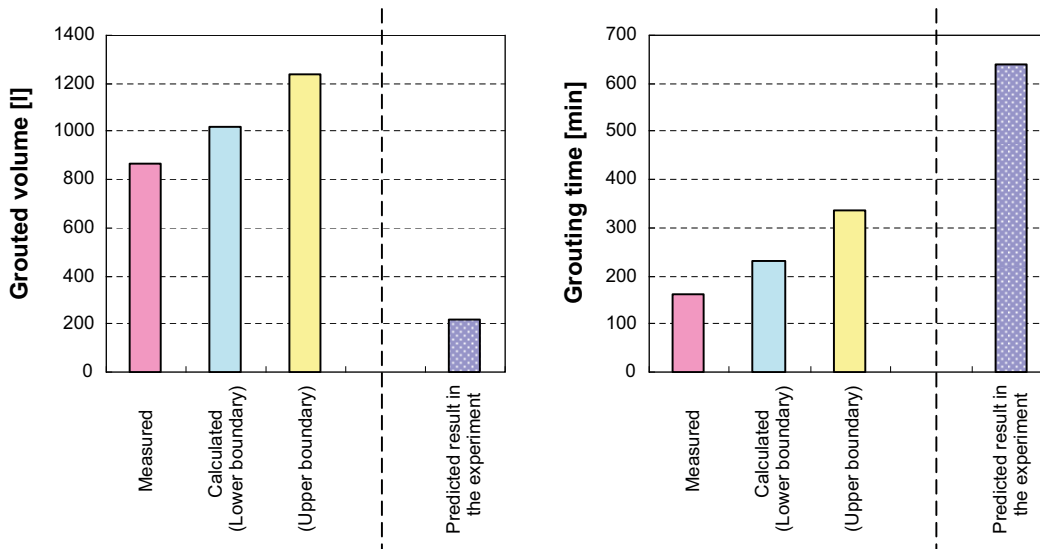
$$b_{wlm} = 1.74 \times b_{inf} \tag{3-4}$$

Figure 3-8. *Comparison of calculated results from hydraulic apertures based on water loss measurement and measured results for Fan 1:1. The graph on the left shows grouted volume, while the graph on the right shows grouting time. The predicted results in the experiment /Emmelin et al. 2004/ are shown on the right in both figures.*
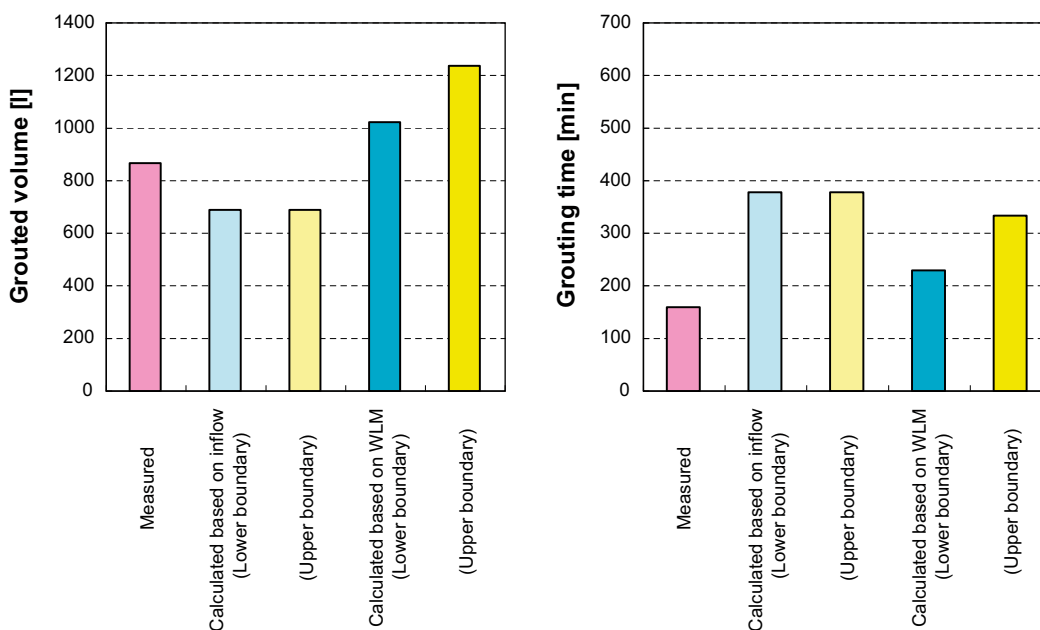

Figure 3-9. *Comparison of calculated results from hydraulic apertures based on inflow and calculated results from hydraulic apertures based on water loss measurement for Fan 1:1. The graph on the left shows grouted volume, while the graph on the right shows grouting time.*

The grouting results calculated using 1.74 times as large hydraulic apertures based on inflow in Fan 1:2 are:

- Lower boundary of total grouted volume excluding filling of the holes   770 litres.
- Upper boundary of total grouted volume excluding filling of the holes   774 litres.
- Lower boundary of grouting time excluding filling of the holes   292 min.
- Upper boundary of grouting time excluding filling of the holes   290 min.

Figure 3-10 shows a comparison between calculated results from 1.74 times as large hydraulic apertures based on inflow and the measured results for Fan 1:2. Figure 3-11 shows a comparison between calculated results from hydraulic apertures based on inflow and results from 1.74 times as large hydraulic apertures. The calculated results for every grouting hole are shown in Appendix F.

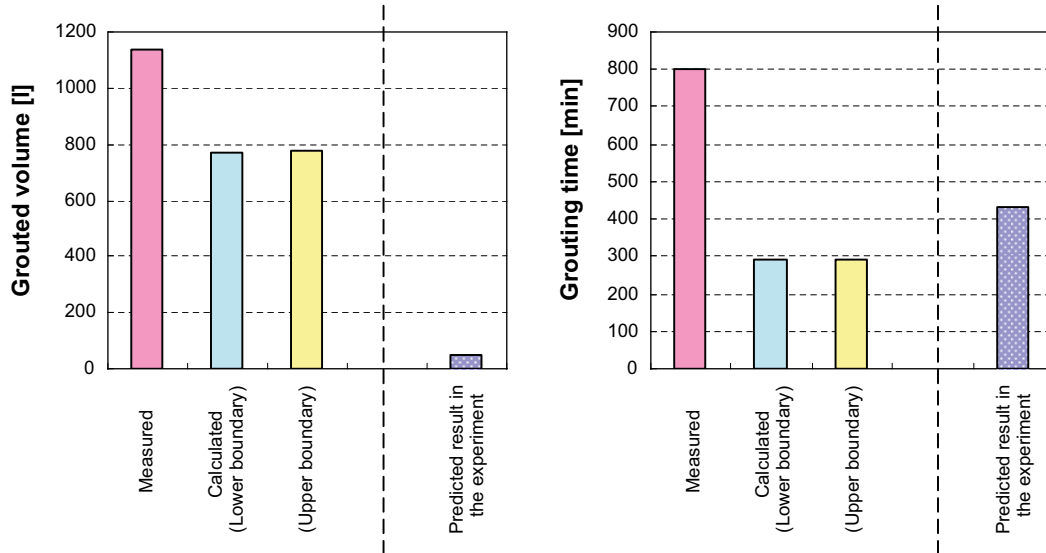In this case both the calculated grouted volume and the calculated grouting time increase.

Figure 3-10. *Comparison of calculated results from 1.74 times as large hydraulic apertures based on inflow and measured results for Fan 1:2. The graph on the left shows grouted volume, while the graph on the right shows grouting time. The predicted results in the experiment /Emmelin et al. 2004/ are shown on the right in both figures.*
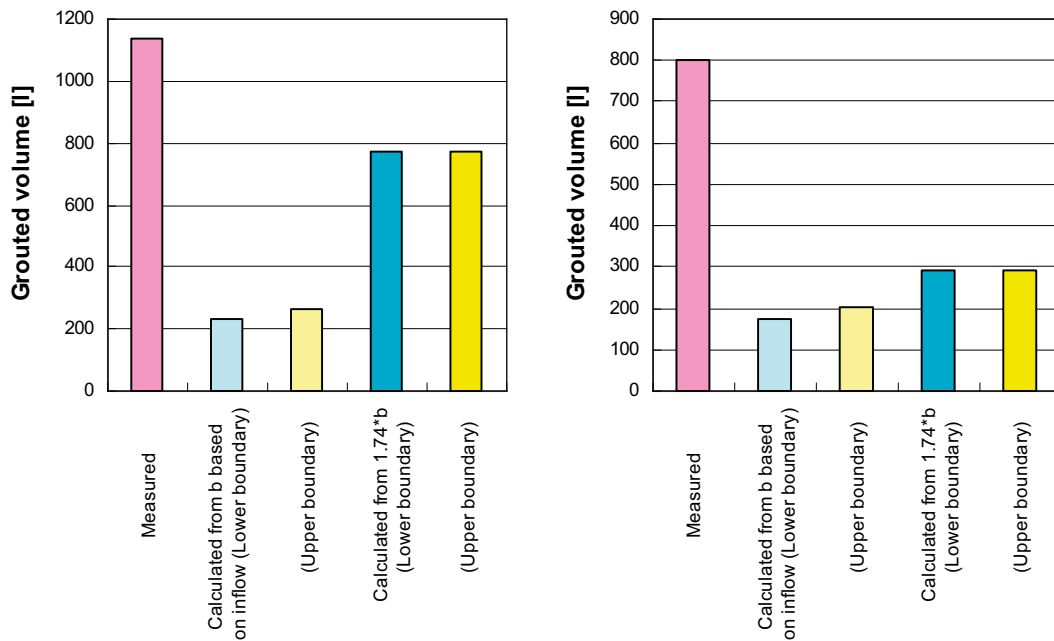

Figure 3-11. *Comparison of calculated results from hydraulic apertures based on inflow and calculated results from 1.74 times as large hydraulic apertures based on inflow for Fan 1:2. The graph on the left shows grouted volume, while the graph on the right shows grouting time.*

The grouting results calculated using 1.74 times as large as hydraulic apertures based on inflow in Fan 2 are:

- Lower boundary of total grouted volume excluding filling of the holes   1,602 litres.
- Upper boundary of total grouted volume excluding filling of the holes   2,143 litres.
- Lower boundary of grouting time excluding filling of the holes   901 min.
- Upper boundary of grouting time excluding filling of the holes   1,837 min.

Figure 3-12 shows a comparison between calculated results from 1.74 times as large hydraulic apertures based on inflow and measured results for Fan 2. Figure 3-13 shows a comparison between calculated results from hydraulic apertures based on inflow and results from 1.74 times as large hydraulic apertures. The calculated results for every grouting hole are shown in Appendix F.

The big difference is found between the upper and the lower boundaries.

3.3.3   Results of additional calculation from changed grouting design

According to the measured grouting data, it would appear that the grouting design for Fan 1:1 was changed during operation as described in 3.1.6. Using the changed grouting design, an additional calculation for Fan 1:1 is made from hydraulic apertures based on both inflow and water loss measurement.
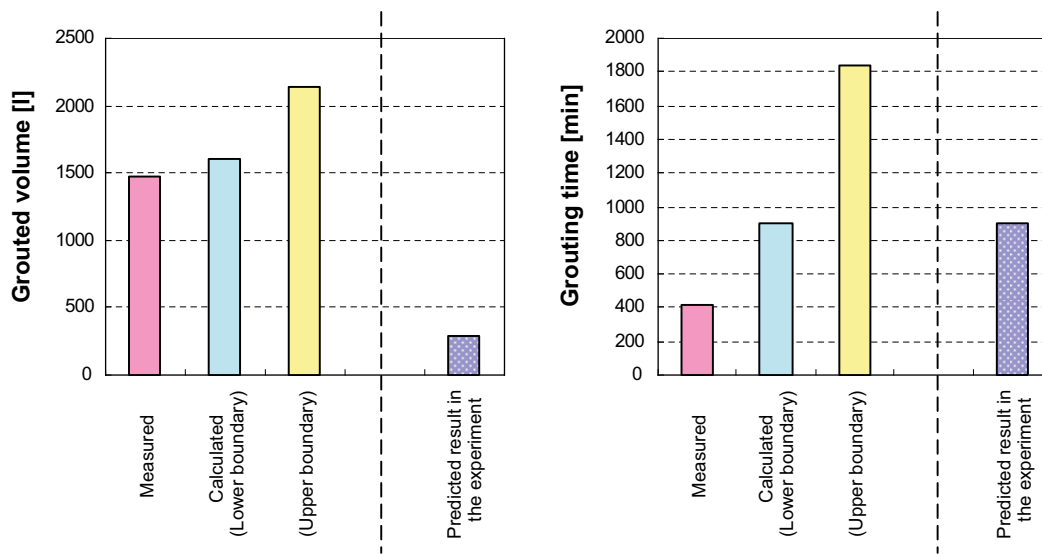

Figure 3-12. *Comparison of calculated results from 1.74 times as large hydraulic apertures based on inflow and measured results for Fan 2. The graph on the left shows grouted volume, while the graph on the right shows grouting time. The predicted results in the experiment /Emmelin et al. 2004/ are shown on the right in both figures.*
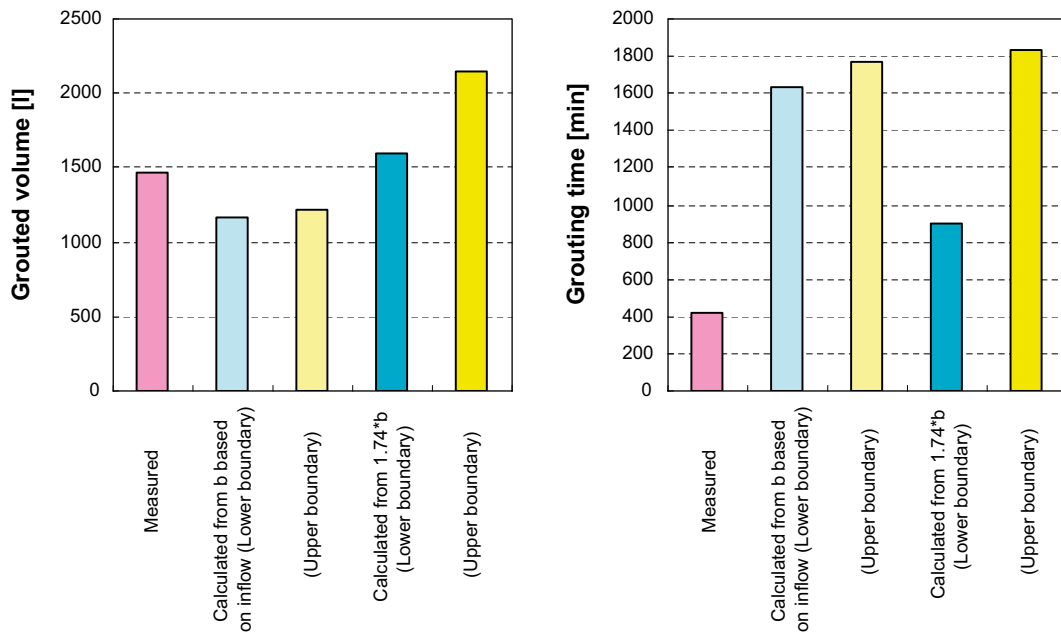
Figure 3-13. *Comparison of calculated results from hydraulic apertures based on inflow and calculated results from 1.74 times as large hydraulic apertures based on inflow for Fan 2. The graph on the left shows grouted volume, while the graph on the right shows grouting time.*

The calculated grouting results from hydraulic apertures based on inflow in Fan 1:1 are:

- Lower boundary of total grouted volume excluding filling of the holes   277 litres.
- Upper boundary of grouting time excluding filling of the holes   151 min.
- Lower boundary of total grouted volume excluding filling of the holes   277 litres.
- Upper boundary of grouting time excluding filling of the holes   151 min.

The calculated grouting results from hydraulic apertures based on water loss measurement in Fan 1:1 are Lower boundary of:

- Lower boundary of total grouted volume excluding filling of the holes   776 litres.
- Upper boundary of total grouted volume excluding filling of the holes   926 litres.
- Lower boundary of grouting time excluding filling of the holes   331 min.
- Upper boundary of grouting time excluding filling of the holes   401 min.

Figure 3-14 shows a comparison between calculated results from hydraulic apertures based on inflow, calculated results from hydraulic apertures based on water loss measurement, and measured results. The calculated results for every grouting hole are shown in Appendix G.

The results are quite interesting. There is no difference between the lower and the upper boundaries of the results based on inflow, but some difference is found in the results based on water loss measurement. The calculated grouting time based on inflow is quite close to the measured time, whereas the calculated grouted volume based on water loss measurement is close to the measured value.
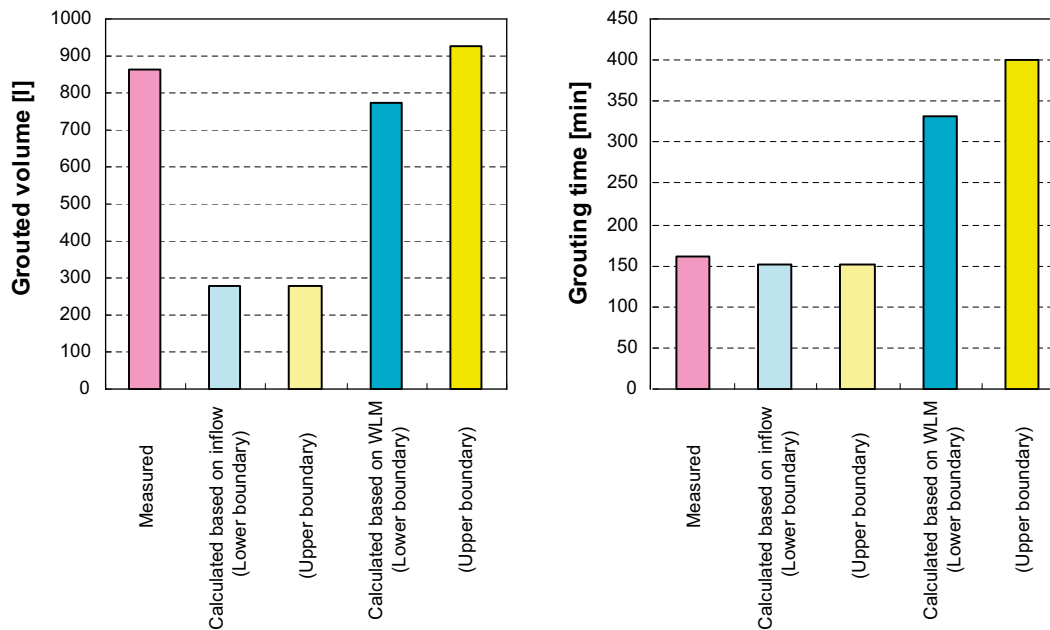
Figure 3-14. *Comparison of calculated results according to the changed grouting design from hydraulic apertures based on inflow, calculated results according to the changed grouting design from hydraulic apertures based on water loss measurement, and measured results for Fan 1:1. The graph on the left shows grouted volume, while the graph on the right shows grouting time. The predicted results in the experiment /Emmelin et al. 2004/ are shown on the right in both figures.*

3.4 Conclusions regarding verification

Figure 3-15 shows the relationship between calculated results from hydraulic apertures based on inflow and results measured for all fans together. The results from the changed grouting design are used for Fan 1:1. Although they are based on the original grouting design, the predicted results in the previous experiment /Emmelin et al. 2004/ noted in 3.1.5 are also plotted in the figures as a reference.

Figure 3-16 shows the relationship between calculated results from hydraulic apertures based on water loss measurement and measured results for all fans together. However, for Fan 1:2 and Fan 2 the calculations are based on 1.74 times as large hydraulic apertures derived from inflow, which are estimated according to the relationship between hydraulic apertures based on inflow and those based on water loss measurement for Fan 1:1, because water loss measurements were not performed in the experiment.

It is found from the figures that:

- Generally the calculated results based on water loss measurement were better at predicting the actual results than those based on inflow.

- The calculated grouting volume based on inflow was much smaller than the measured value.

- The calculated grouting volume based on water loss measurement was an accurate prediction.

- The difference between the upper and the lower boundaries of the result based on inflow was very little.

- In Fan 2 the calculated results based on water loss measurement varied widely.

- The lower boundary of the calculated result based on water loss measurement was close to the measured value.
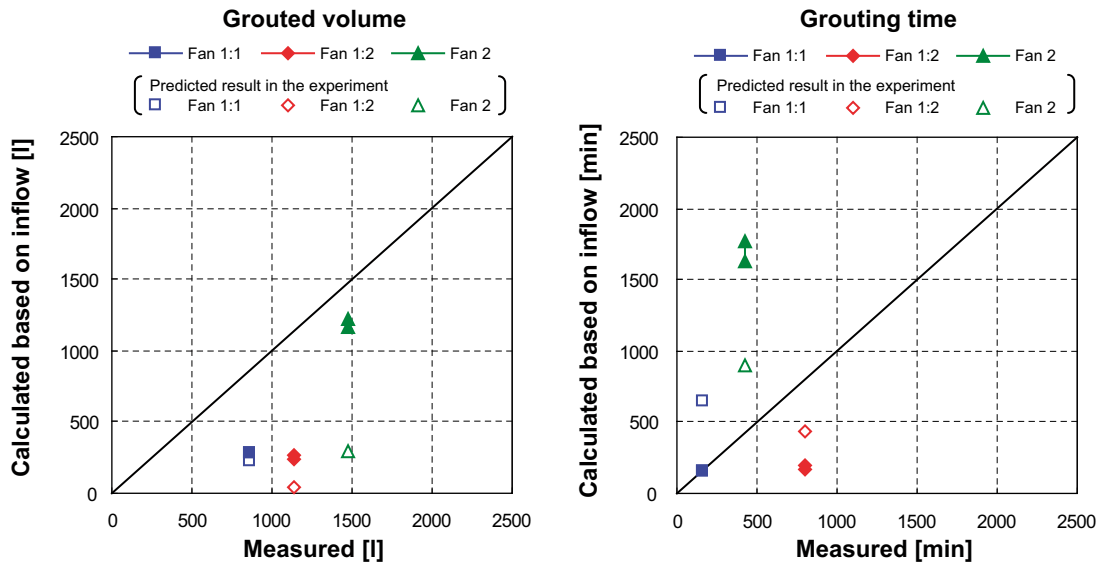
Figure 3-15. *Relationship between calculated results from hydraulic apertures based on inflow and measured results for all fans. The graph on the left shows grouted volume, while the graph on the right shows grouting time. The calculated results consist of the lower and the upper boundaries. The predicted results in the experiment /Emmelin et al. 2004/ are also shown together.*
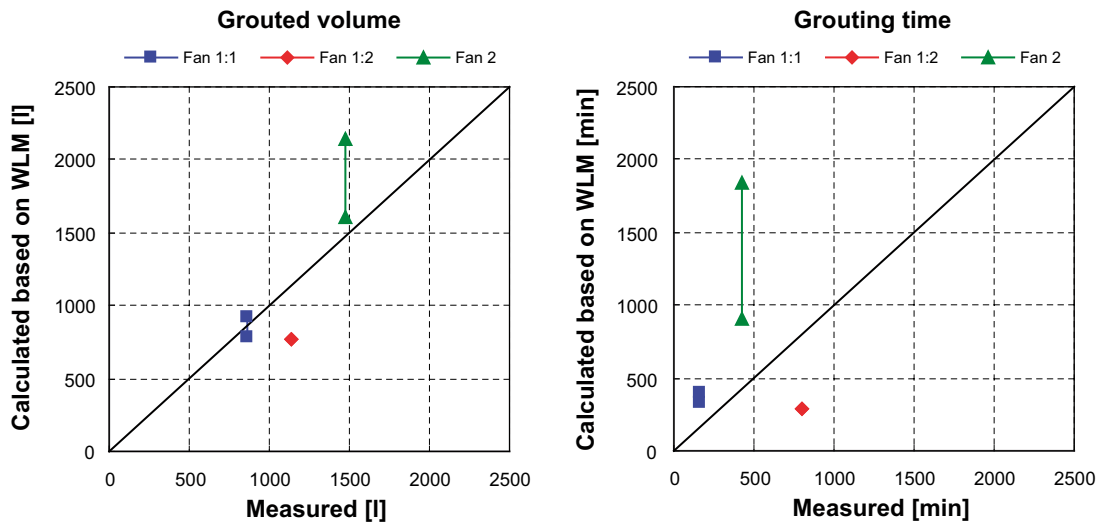

Figure 3-16. *Relationship between calculated results from hydraulic apertures based on water loss measurement or from 1.74 times as large hydraulic apertures based on inflow and measured results for all fans. The graph on the left shows grouted volume, while the graph on the right shows grouting time. The calculated results consist of the lower and upper boundaries.*

The conclusion of the verification can be summarized as follows:

• The calculated results based on water loss measurement were better at predicting the actual results than those based on inflow. In particular, the calculated grouting volume based on water loss measurement was an accurate prediction. However, in Fan 1:1 the calculated grouting time based on inflow was closer to the measured result than the value based on water loss measurement. This would indicate the importance of a deeper understanding of hydraulic aperture and an adequate fracture interpretation.

- There was a big difference in the results based on water loss measurement in Fan 2 between the upper and the lower boundaries of the grouting result for changed grout mixes. This can be explained as follows: the greater the volume of the first grout, the greater the impact of the grout on the second grouting. The upper boundary of the grouting result (grouted volume and grouting time) based on water loss measurement in Fan 2 was much higher than the measured result, whereas the lower boundary was close to the measured result. It can be concluded that the assumption for calculating the upper boundary, that the properties of the first grout are the same as those of the groundwater, was unrealistic for this case and that the assumption for calculating the lower boundary, that the properties of the first grout are the same as those of the second grout, was close to the actual grouting situation. In order to evaluate the effect of changing grout mixes more accurately, a better approximation of the solution for changing grout mixes should be sought.

- Though there is still room for further improvement of the theory as noted above, it is concluded that the further developed theory is well verified and can be applied to grouting design and analysis.

4 Analysis of different stop criteria

4.1 Introduction

Although theoretical studies of rock grouting and analytical researches of grouting data have been carried out, stop criteria for grouting have mainly been based on practical knowledge, such as:

- Grouting is completed when the grout flow is less than a certain value at maximum pressure.

- Grouting is completed when the grout take is above a certain value.

Since these empirically based stop criteria are not related to grout penetration, the grouting result may be inadequate or uneconomical. However, by use of the further developed and verified theory, stop criteria can be designed based directly on grout penetration, such as:

- Grouting is completed when the grout penetration is above a certain value.

Three types of stop criteria – one based on grout flow, one on grout take and the third on grout penetration – are compared by calculating the grouting results obtained from application of the theory. The calculations are carried out for both 1D and 2D flows. Three types of hypothetical rock masses with different permeability are used for the calculations.

4.2 Calculation models

4.2.1 Hypothetical rock types

The rock type used for the calculations is defined by the number of fractures and the aperture of the fractures in a grouting hole. It is assumed that the aperture distribution is described by a Pareto distribution /Gustafson and Fransson 2006/. For the 1D case it is assumed that the width of the fracture is 1 metre.

Rock type A is low permeable. The fractures have an aperture of between 0.05 and 0.1 mm. The total number of fractures is 3/hole and the transmissivity calculated by the cubic law is $7.9 \cdot 10^{-7}$ m²/s. The corresponding Lugeon value calculated by (3-3), assuming that the length of the test section is 15 m and the radius of the borehole is 32 mm, is 0.3. The distribution of the fracture apertures for rock type A is shown in Figure 4-1 and Table 4-1.
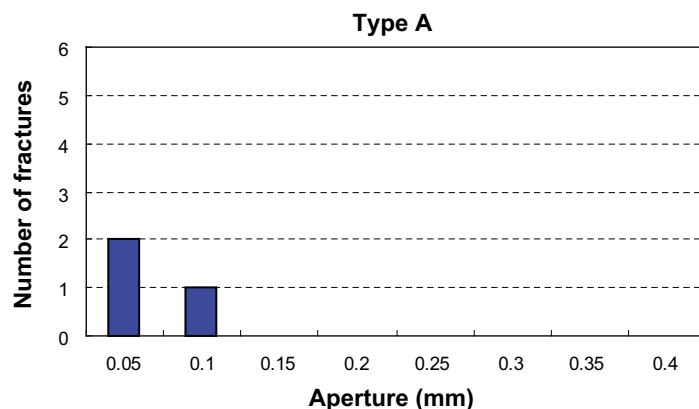

Figure 4-1. *Number of fractures with different apertures in a grouting hole for rock type A.*

Table 4-1. Hydrogeological properties for rock type A, B and C.

Type	Permeability	Number of fractures	Mean aperture (mm)	Max. aperture (mm)	Transmissivity (m²/s)	Lugeon value* (Lu)
A	low	3	0.067	0.100	7.9E–07	0.3
B	medium	8	0.094	0.200	8.7E–06	3.6
C	high	11	0.123	0.300	3.6E–05	14.8

* the corresponding Lugeon value is calculated by assuming that the length of the test section is 15 m and the radius of the borehole is 32 mm.

Rock type B is medium permeable. The fractures have an aperture of between 0.05 and 0.2 mm. The total number of fractures is 8/hole, the transmissivity is $8.7 \cdot 10^{-6}$ m²/s, and the corresponding Lugeon value is 3.6. The distribution of the fracture apertures for rock type B is shown in Figure 4-2 and Table 4-1.

Rock type C is highly permeable. The fractures have an aperture between 0.05 and 0.3 mm. The total number of fractures is 11/hole, the transmissivity is $3.6 \cdot 10^{-5}$ m²/s, and the corresponding Lugeon value is 14.8. The distribution of the fracture apertures for rock type C is shown in Figure 4-3 and Table 4-1.
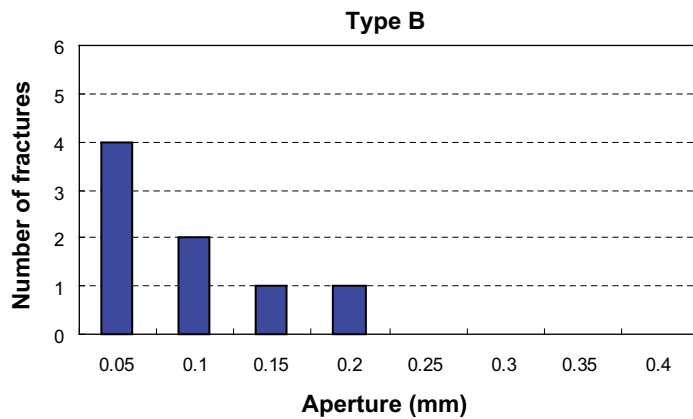

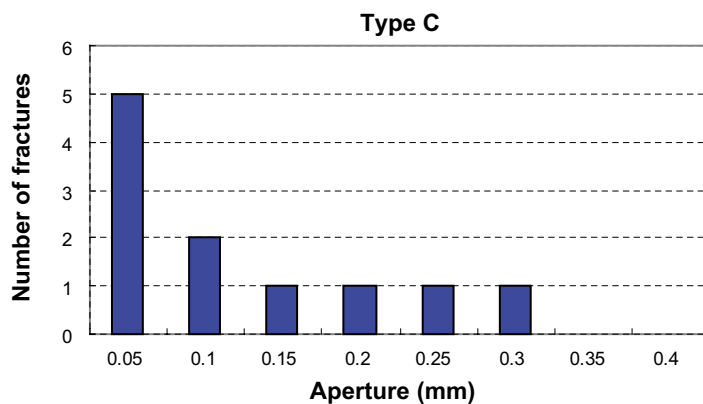***Figure 4-2.*** *Number of fractures with different apertures in a grouting hole for rock type B.*

Figure 4-3. *Number of fractures with different apertures in a grouting hole for rock type C.*

4.2.2 Grouting design

The grouting results based on three different stop criteria are compared for rock types A, B and C. The three types of stop criteria used for the calculation are:

- Grout penetration is above 10 m for the minimum groutable aperture.
- Grout flow is less than 1 litre/min.
- Grout take is above 1,500 litres.

The same grouting design, except for the stop criteria, is used for all calculations for rock types A, B and C. The basic grouting design is based on the same properties as the example in the /Gustafson and Stille 2005/, which are:

- Grouting pressure   2.4 MPa above groundwater pressure.
- Grout properties   Yield value (τ_0): 1.4 Pa, Viscosity (μ_g): 0.02 Pas, Minimum groutable aperture ($b_{groutable}$): 0.1 mm.
- Grouting equipment capacity   Maximum grout flow (Q_{max}): 20 litres/min.

4.2.3 Calculation

The calculations are done for 18 combinations of the 1D and 2D cases, three rock types and three stop criteria. Figure 4-4 shows an example of the results of a calculation for the grouting design based on grout penetration. In this case the grout flow is limited to 20 litres/min. by the capacity of the grouting equipment for the first several seconds. After the grouting pressure reaches 2.4 MPa, the grout flow starts to decrease and grouting is completed when the grout penetration is greater than 10 m.
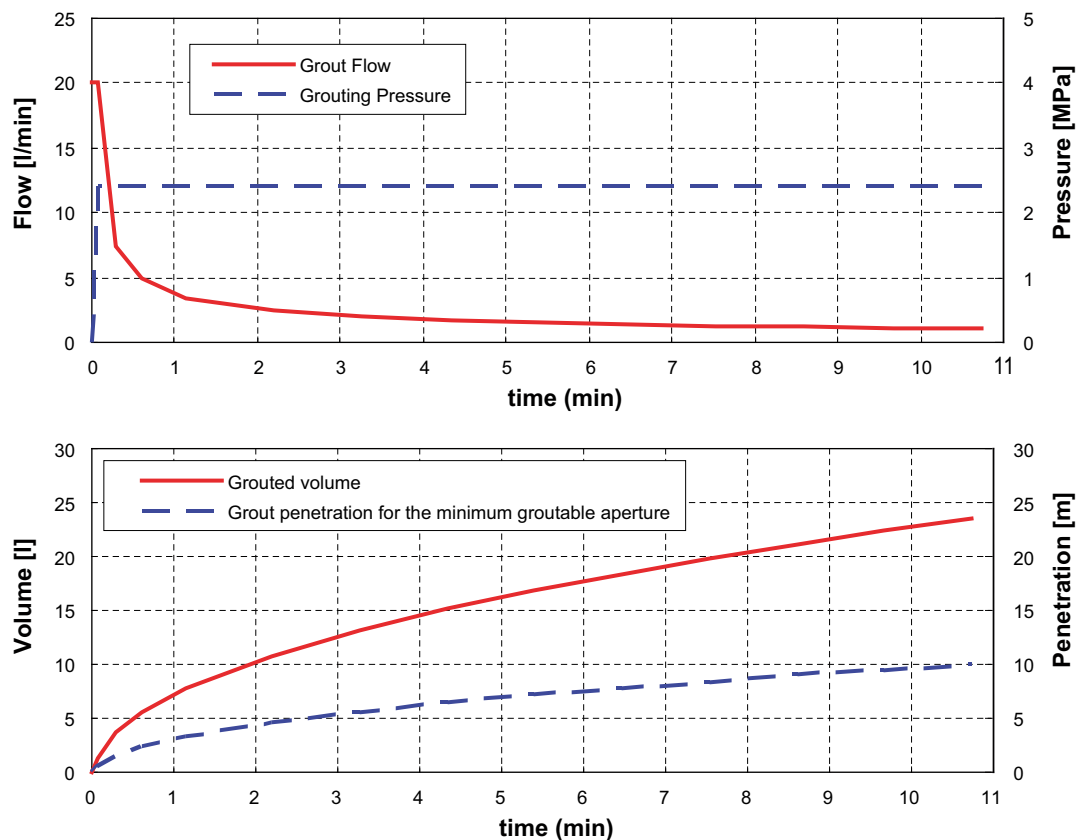

Figure 4-4. *An example of a calculation for the grouting design based on grout penetration (1D, rock type C). The top graph shows the grout flow and the grouting time. The bottom graph shows the grouted volume and the grout penetration for the minimum groutable aperture.*

4.3 Results

4.3.1 Comparison of calculated results

The calculated results used for the comparison comprise:

- Grout penetration for the minimum groutable aperture.
- Grouting time.
- Grouted volume.
- Final grout flow when grouting is completed.

Figure 4-5 shows a comparison of calculated results for the 1D case based on three different stop criteria. Great differences are found between all the results derived from the three stop criteria.

For the stop criteria based on grout penetration (l>10 m), it is natural that the calculated grout penetration for the minimum aperture is exactly 10 metres for all rock types. Since the time scale is not a function of the fracture aperture as shown in (2-4), (2-5), the calculated grouting time is the same for all rock types. Higher permeability results in higher calculated grouted volume and final grout flow.
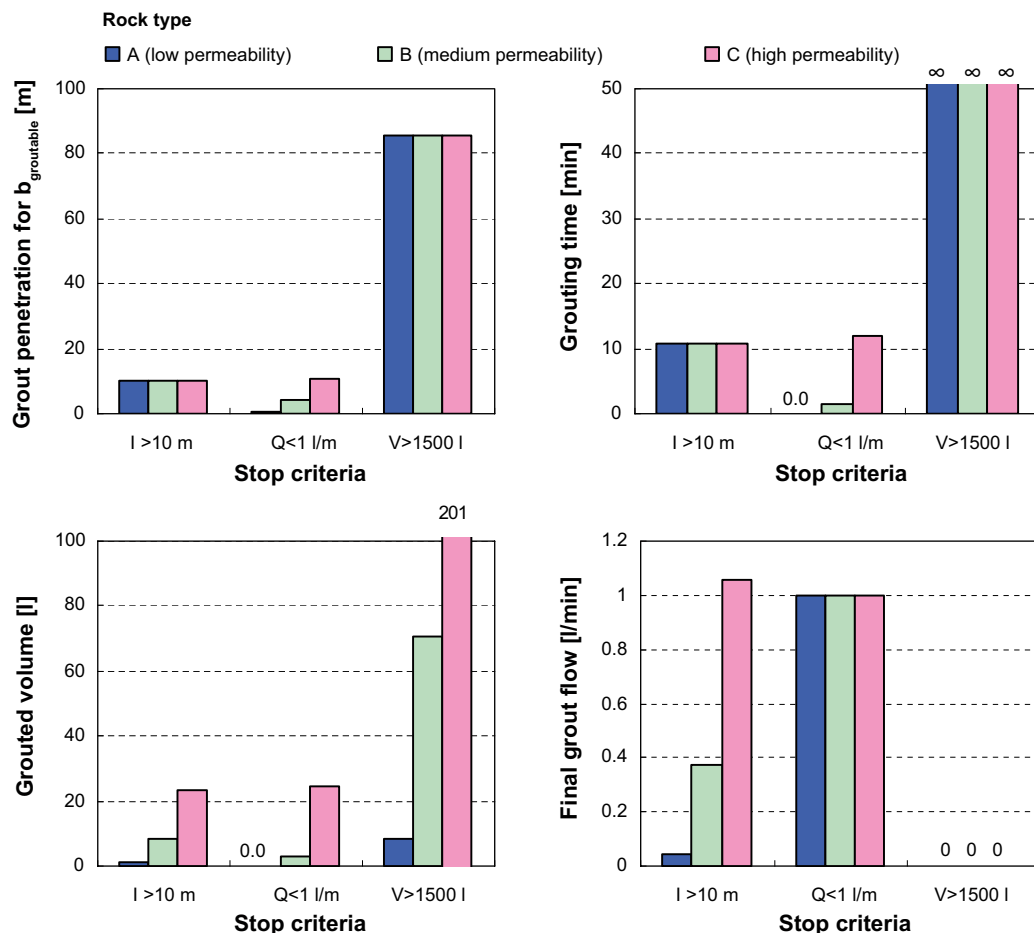

Figure 4-5. *Comparison of calculated results for the 1D case based on three different stop criteria. "l>10 m" shows the stop criteria that the grout penetration is greater than 10 m for the minimum groutable aperture, "Q<1 l/m" shows that the grout flow is less than 1 liter/min, and "V>1,500 l" shows that the grout take is greater than 1,500 litres.*

For the stop criteria based on grout flow (Q<1 l/m), the calculated grouting results are dependent on the rock types except for the final grout flow, which must be 1 litre/min. Higher permeability results in higher calculated grouting time and grouted volume.

Grouting with the stop criteria based on grouted volume (V>1,500 l) is not completed for all three rock types because the maximum grouted volume is less than 1,500 litres.

Great differences are found between all the results derived from the three stop criteria. The results show the importance of choosing the theoretically based stop criteria in order to avoid inadequate or uneconomical grouting.

Figure 4-6 shows a comparison of calculated results for the 2D case based on three different stop criteria. For the 2D case, much greater differences are also found between all the results derived from three stop criteria.

For the stop criteria based on grout penetration (l>10 m), as in the 1D case, it is natural that the calculated grout penetration for the minimum aperture is exactly 10 metres for all rock types. However, the calculated grouting time for rock type C is longer than for other rock types because the grout flow is limited to the capacity of the grouting equipment for rock type C. Higher permeability results in higher calculated grouted volume and final grout flow, but they are much higher than those for the 1D case.
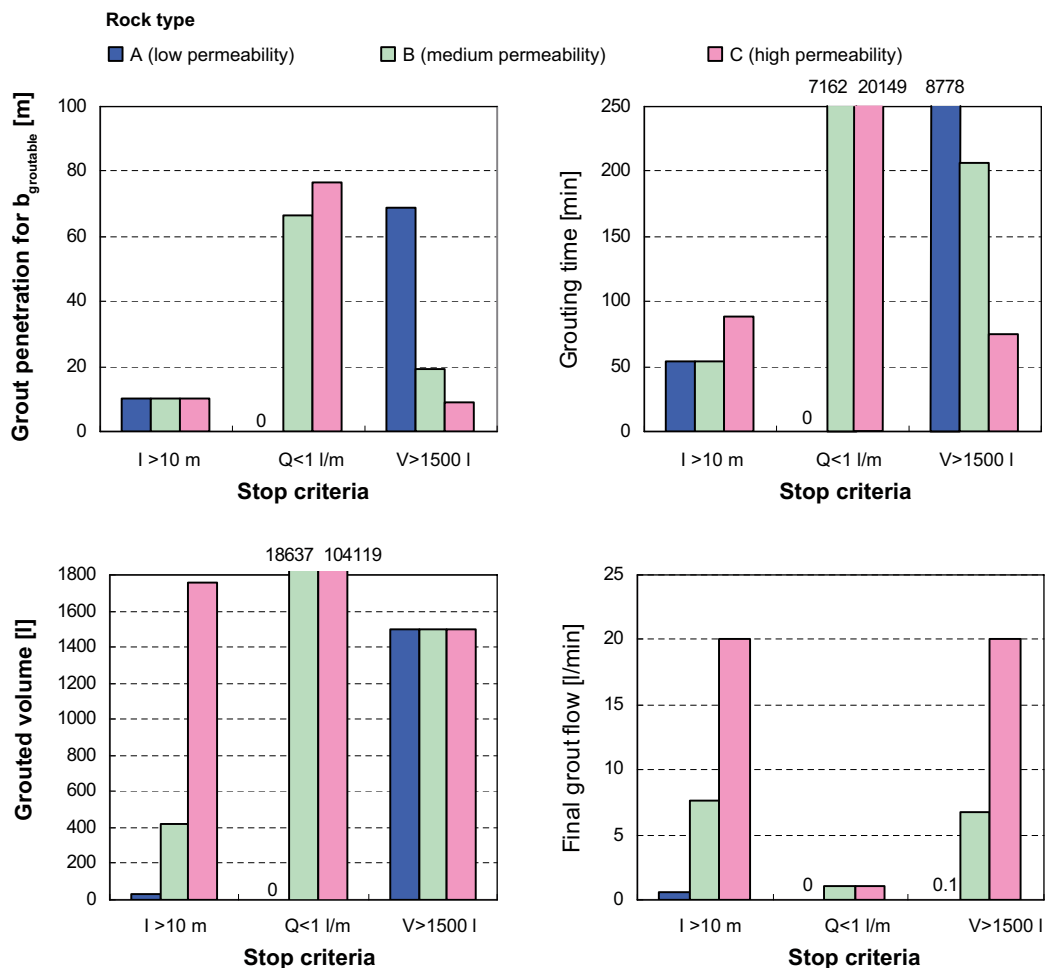

Figure 4-6. *Comparison of calculated results for the 2D case based on three different stop criteria. "l>10 m" shows that the grout penetration is greater than 10 m for the minimum groutable aperture, "Q<1 l/m" shows that the grout flow is less than 1 liter/min, and "V>1,500 l" shows that the grout take is greater than 1,500 litres.*

For the stop criteria based on grout flow (Q<1 l/m), the calculated grouting results are dependent on the rock types with the exception of the final grout flow, which must be 1 litre/min. However, no grout is injected for rock type A because the transmissivity is too low to afford more than 1 litre/minute grout flow. Compared to the 1D case, the calculated grouting time and grouted volume are extremely high.

For the stop criteria based on grouted volume (V>1,500 l), higher permeability results in lower calculated grout penetration and grouting time, but they are also very high compared to the 1D case.

For the 2D case, greater differences are found between all the results derived from the three stop criteria. The results show the greater importance of choosing the theoretically based stop criteria in order to avoid inadequate or uneconomical grouting.

Furthermore, it is found that in general, the results for the 2D case are much higher than those for the 1D case, so estimating the flow dimension of the fracture system is important.

4.3.2   Calculated results on fracture level

As described in 4.3.1, the calculated grouting results are dependent on the fracture apertures. Therefore, even if the stop criteria are based on grout penetration, the calculated grout volume is very high for highly permeable rock types. Figure 4-7, Figure 4-8 and Figure 4-9 show the number of fractures, the calculated grout penetration and the calculated grouted volume for different apertures for rock types A, B and C in the 1D case.

It is found that grout penetration is proportional to fracture aperture. Greater penetration requires wider apertures in order that grout penetration will be above 10 m for the minimum groutable aperture. This tendency is high for rock type C.
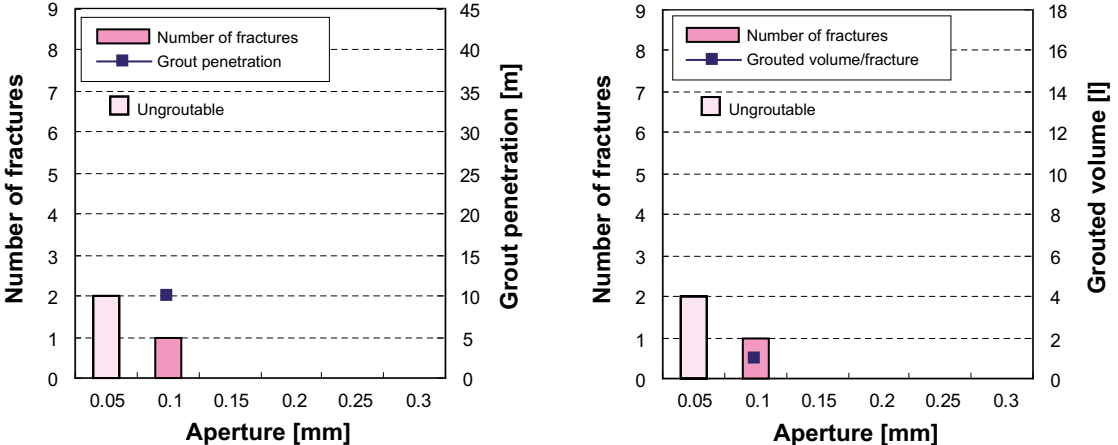

Figure 4-7. *Calculated results for low permeable rock type A in the 1D case based on the stop criteria that the grout penetration is greater than 10 m for the minimum groutable aperture. The graph on the left shows the number of fractures and the grout penetration for each aperture. The graph on the right shows the number of fractures and the grouted volume for each aperture.*

Figure 4-8. *Calculated results for medium permeable rock type B in the 1D case based on the stop criteria that the grout penetration is greater than 10 m for the minimum groutable aperture. The graph on the left shows the number of fractures and the grout penetration for each aperture. The graph on the right shows the number of fractures and the grouted volume for each aperture.*
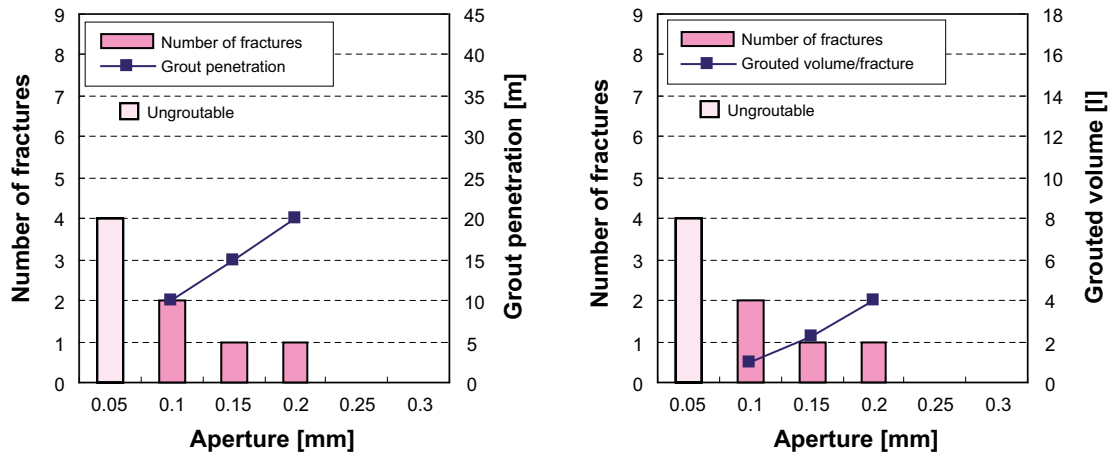

Figure 4-9. *Calculated resulst for highly permeable rock type C in the 1D case based on the stop criteria that the grout penetration is greater than 10 m for the minimum groutable aperture. The graph on the left shows the number of fractures and the grout penetration for each aperture. The graph on the right shows the number of fractures and the grouted volume for each aperture.*
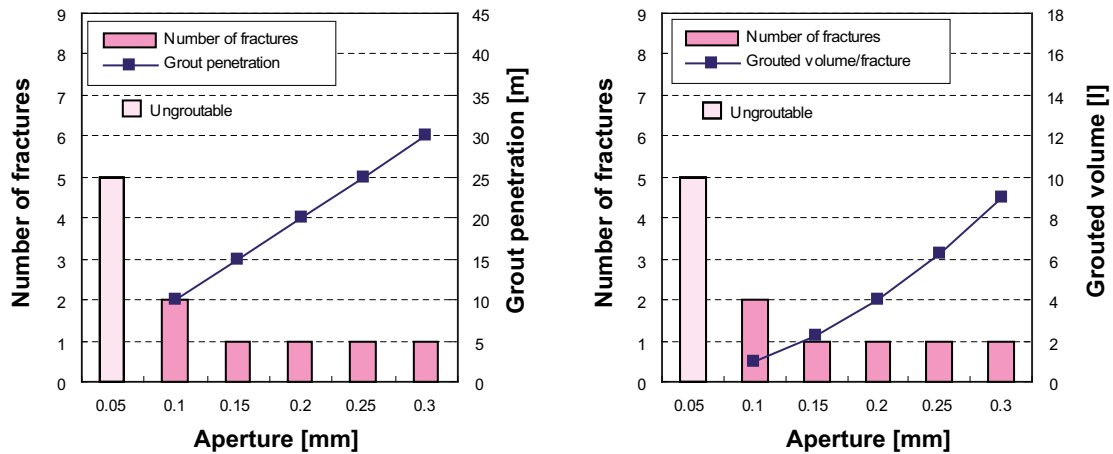
Figure 4-10, Figure 4-11 and Figure 4-12 show the number of fractures, the calculated grout penetration and the calculated grouted volume for different apertures for rock types A, B and C in the 2D case.

It is found that, as in the 1D case, grout penetration is proportional to fracture aperture. However, wider apertures give much greater calculated grouted volumes.
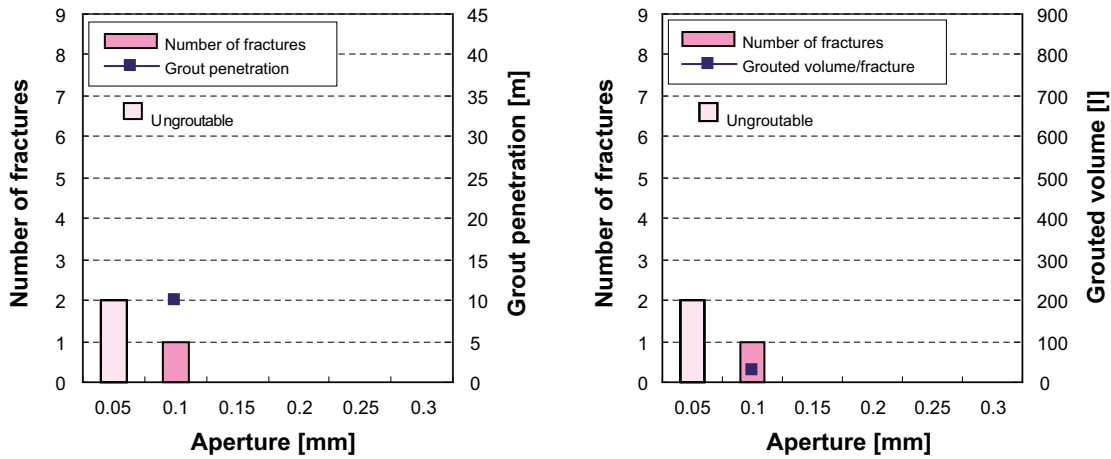
Figure 4-10. *Calculated results for low permeable rock type A in the 2D case based on the stop criteria that the grout penetration is greater than 10 m for the minimum groutable aperture. The graph on the left shows the number of fractures and the grout penetration for each aperture. The graph on the right shows the number of fractures and the grouted volume for each aperture.*

Figure 4-11. *Calculated results for medium permeable rock type B in the 2D case based on the stop criteria that the grout penetration is greater than 10 m for the minimum groutable aperture. The graph on the left shows the number of fractures and the grout penetration for each aperture. The graph on the right shows the number of fractures and the grouted volume for each aperture.*
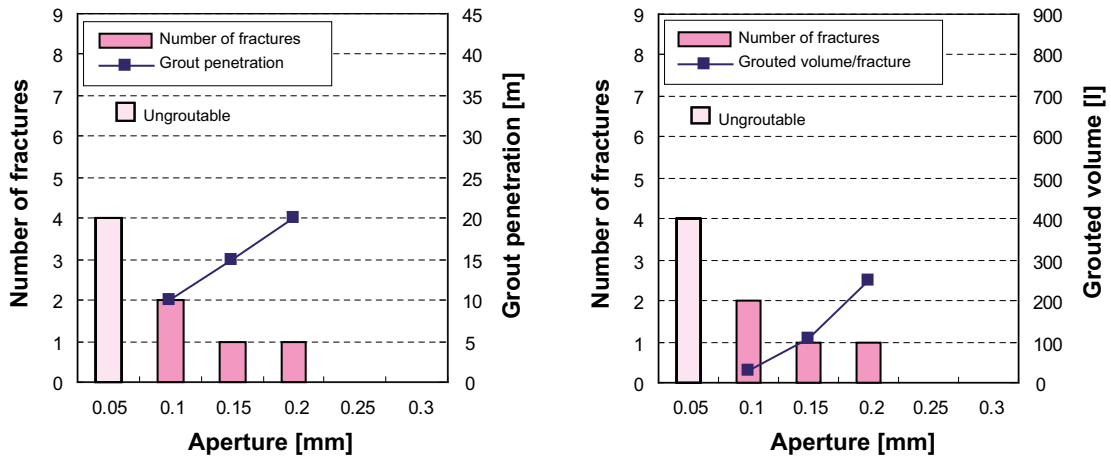
In order to prevent excessive spreading of the grout for wider apertures, a new different grouting design is necessary. One example is to carry out grouting in two grouting rounds. A simple calculation is carried out using the same grouting design with stop criteria based on grout penetration, with the exception of the minimum groutable aperture, which is:

- Minimum groutable aperture ($b_{groutable}$): 0.2 mm for the first grouting round.
- Minimum groutable aperture ($b_{groutable}$): 0.1 mm for the second grouting round.

The calculation is carried out for rock type C in the 2D case. The calculated grouting results from using one grouting round are:

- Total grouted volume excluding filling of the holes   1,759 litres.
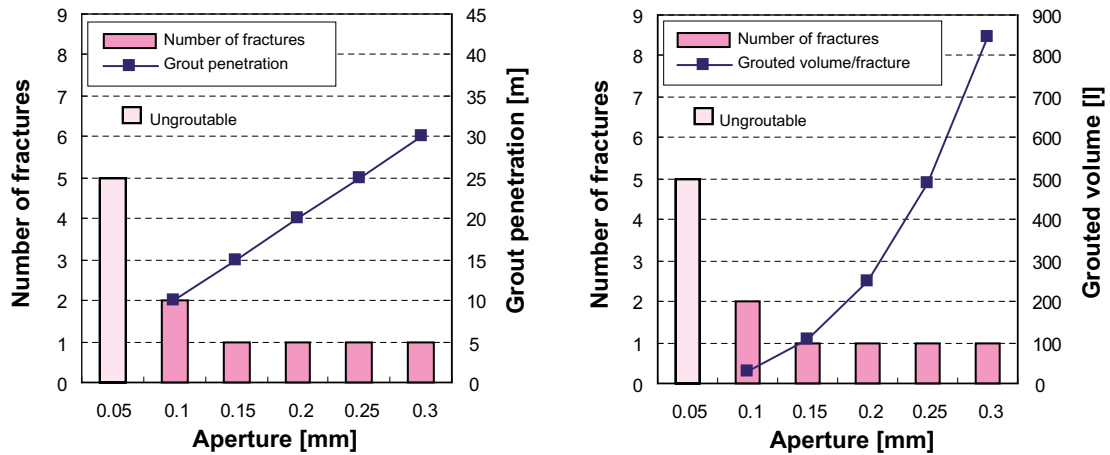- Grouting time excluding filling of the holes   88 min.

Figure 4-12. Calculated resulst for highly permeable rock type C in the 2D case based on the stop criteria that the grout penetration is greater than 10 m for the minimum groutable aperture. The graph on the left shows the number of fractures and the grout penetration for each aperture. The graph on the right shows the number of fractures and the grouted volume for each aperture.

The calculated grouting results from using two grouting rounds are:

- Total grouted volume excluding filling of the holes   567 litres.
- Grouting time excluding filling of the holes   73 min.

The calculated results for the first round are shown in Figure 4-13. The calculated results for the second round are shown in Figure 4-14. Figure 4-15 shows a comparison between calculated results using one grouting round and two grouting rounds.

Both total grouted volume and grouting time are lower when two grouting rounds are used than one grouting round. Of course, grouting with two grouting rounds takes more time besides the grouting time, but using two grouting rounds is better in terms of grouted volume. Moreover, the theoretical design based on grout penetration is very useful for choosing a good grouting design.

Figure 4-13. Calculated results of the first grouting round for highly permeable rock type in the 2D case based on the stop criteria that the grout penetration is greater than 10 m for the minimum groutable aperture. The graph on the left shows the number of fractures and the grout penetration for each aperture. The graph on the right shows the number of fractures and the grouted volume for each aperture.
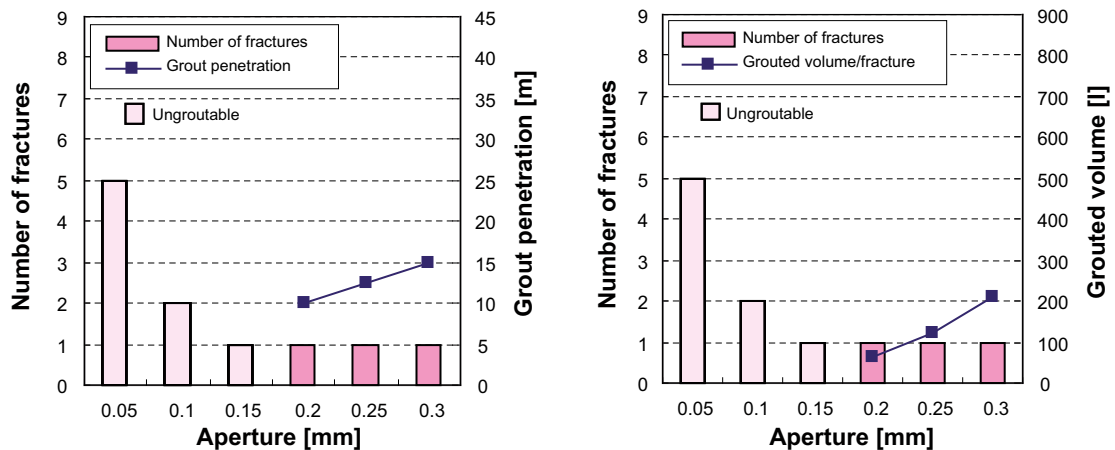
Figure 4-14. *Calculated results of the second grouting round for highly permeable rock type in the 2D case based on the stop criteria that the grout penetration is greater than 10 m for the minimum groutable aperture. The graph on the left shows the number of fractures and the grout penetration for each aperture. The graph on the right shows the number of fractures and the grouted volume for each aperture.*
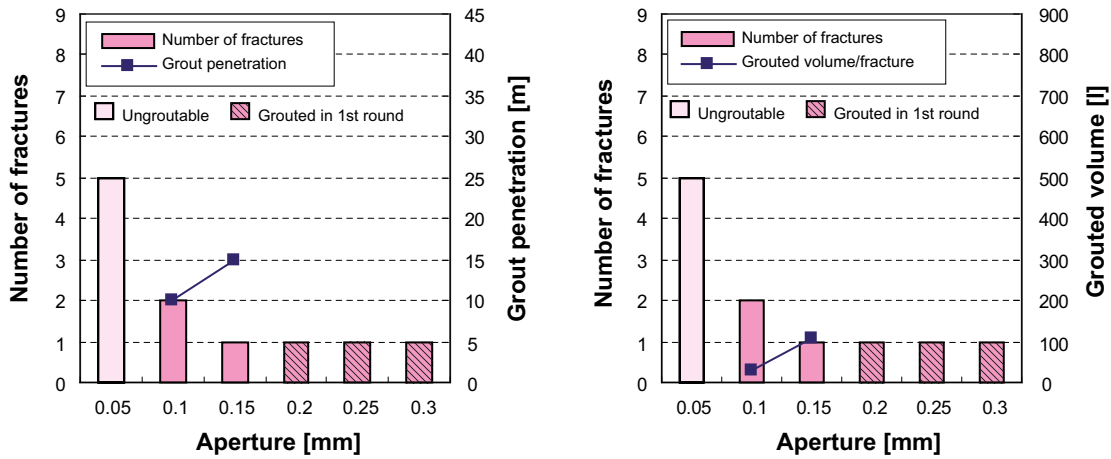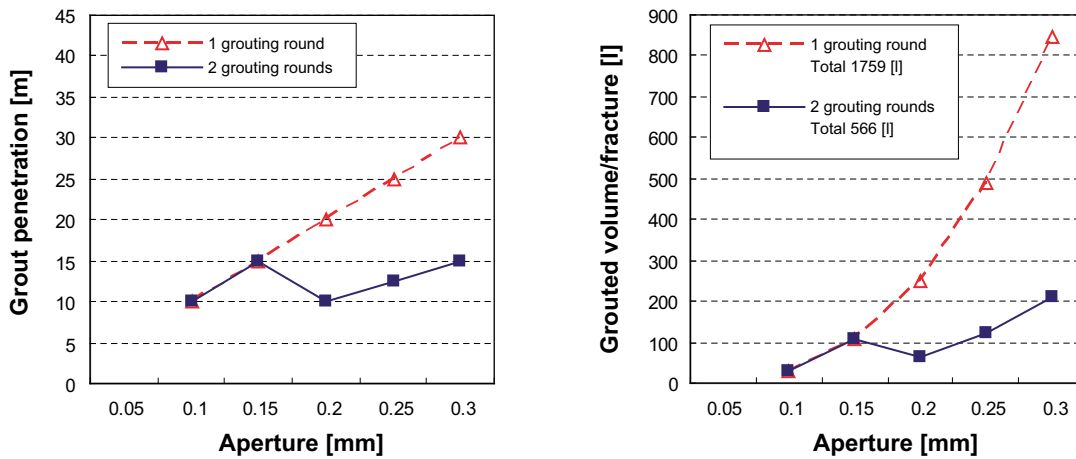

Figure 4-15. *Comparison between calculated results using one grouting round and using two grouting rounds for highly permeable rock type in the 2D case based on the stop criteria that the grout penetration is greater than 10 m for the minimum groutable aperture. The graph on the left shows the grout penetration for each aperture. The graph on the right shows the grouted volume for each aperture.*

4.4 Conclusions

Three types of stop criteria – one based on grout flow, one on grout take, and the third on grout penetration – are compared by calculating the grouting results obtained from application of the theory. The calculations are carried out for both 1D and 2D flows. Three types of hypothetical rock masses with different permeabilities are used for the calculations. Of course, the results are dependent on what values are set as stop criteria, but they indicate the importance of the theoretical design based on grout penetration.

The conclusions of the analysis of different stop criteria can be summarized as follows:

- For the stop criteria based on grout penetration, the calculated grouting time is same for all rock types if the grout flow is lower than the capacity of the grouting equipment. Higher permeability results in higher calculated grouted volume and final grout flow.

- For the stop criteria based on grout flow, higher permeability results in higher calculated grout penetration, grouting time and grouted volume.

- For the stop criteria based on grouted volume, higher permeability results in lower calculated grout penetration, lower calculated grouting time and higher calculated final grout flow if the maximum grouted volume is not less than the required grouted volume.

- Great differences are found between all the results derived from the three stop criteria for both the 1D and 2D cases. The results show the importance of choosing the theoretically based stop criteria in order to avoid inadequate or uneconomical grouting.

- In general, both grouted volume and grouting time for the 2D case are much higher than those for the 1D case. It is important to estimate the flow dimension of the fracrture system.

- Grout penetration is proportional to fracture aperture. Greater penetration requires wider apertures in order to achieve the required penetration for the minimum groutable aperture.

- In order to prevent excessive spreading of the grout for wider apertures in highly permeable rock types, using the grouting design with two grouting rounds is one solution. A simple calculation shows that both total grouted volume and grouting time are lower when two grouting rounds are used than when one grouting round is used.

- The theoretical design based on grout penetration is very useful for choosing a good grouting design. Furthermore, the further developed theory is widely applicable to various grouting methods and makes it easy to calculate the grouting results.

5 Parameter analysis

5.1 Introduction

The method of parameter analysis is to compare the calculated results derived from different grouting parameters by using the further developed theory. Parameter analysis is important because:

- It can be a guide in choosing the theoretically most suitable grouting design from among many different grouting strategies.

- It can demonstrate the influence of changes in grouting parameters, for example grout properties, during the grouting operation.

- It can demonstrate the difference between the results derived from different rock masses.

The effect of variations in grouting parameters such as grouting pressure and grout materials is evaluated by calculating the grouting results obtained from application of the theory. The calculations are done for both 1D and 2D flows. Three types of hypothetical rock masses with different permeabilities are used for the calculations.

5.2 Calculation models

5.2.1 Hypothetical rock types

Three types of rock masses are used for the calculations. Rock type A is low permeable, rock type B is medium permeable and rock type C is highly permeable. These rock types are same as shown in 4.2.1.

5.2.2 Grouting design

The basic grouting design in the reference case is shown below:

- Grouting pressure   2.4 MPa above groundwater pressure.

- Grout properties   Yield value (τ_0): 1.4 Pa, Viscosity (μ_g): 0.02 Pas, Minimum groutable aperture ($b_{groutable}$): 0.1 mm.

- Grouting equipment capacity   Maximum grout flow (Q_{max}): 20 liters/min.

- Stop criteria   Grout penetration is above 10 m for the minimum groutable aperture.

This is the same as the grouting design with the stop criteria based on grout penetration shown in 4.2.2 and is used for calculation as a reference case.

5.2.3 Calculation cases

The calculations are carried out for 42 combinations of the 1D and 2D cases, three rock types and different grouting parameters such as:

- Reference case.

- Double and one-half grouting pressure.

- Double and one-half yield strength.

- Double and one-half viscosity.

5.3 Results

5.3.1 Calculated results used for the comparison

The calculated results used for the comparison are:

• Grouting time.

• Final grout flow when grouting is completed.

High permeability gives high calculated grouted volume, but the grouted volume is not dependent on grouting parameters such as grouting pressure and grout properties because the stop criterion is based on grout penetration and is the same for different grouting parameters.

5.3.2 Effect of variations in grouting pressure

Figure 5-2 and Figure 5-3 show the relationship between grouting pressure and calculated results for the 1D and 2D cases, respectively.

For the 1D case, the calculated grouting time is inversely proportional to the grouting pressure, and there is no difference between the calculated grouting times derived from different rock types. However, the calculated final grout flow is proportional to the grouting pressure and high permeability results in high final grout flow.

The same can be said for the 2D case, except for rock type C. This difference is due to the capacity of the grouting equipment. Since the grout flow is limited to the capacity, the calculated grouting time is longer. The grouting time and the final grouting flow are dependent on the capacity of the grouting equipment in highly permeable rock.
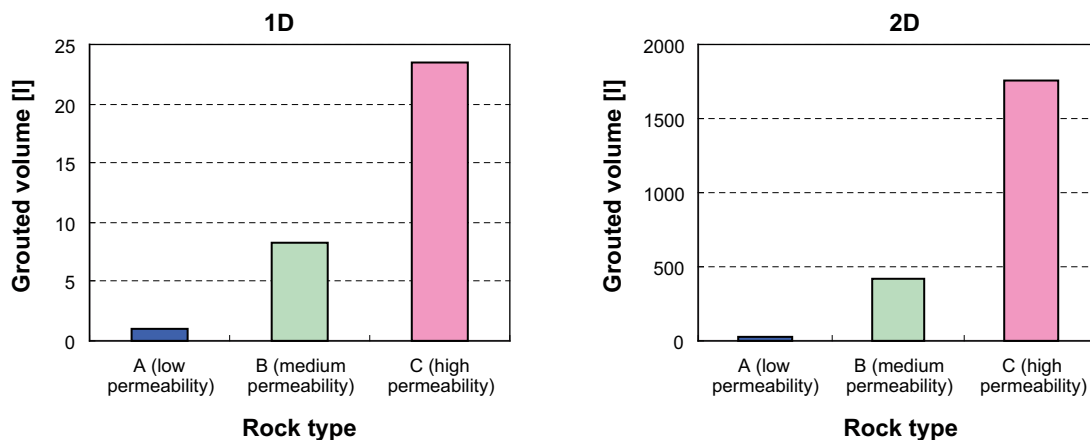

Figure 5-1. *Calculated grouted volume. The graph on left shows the results for 1D case, while the graph on the right shows the results for the 2D case.*
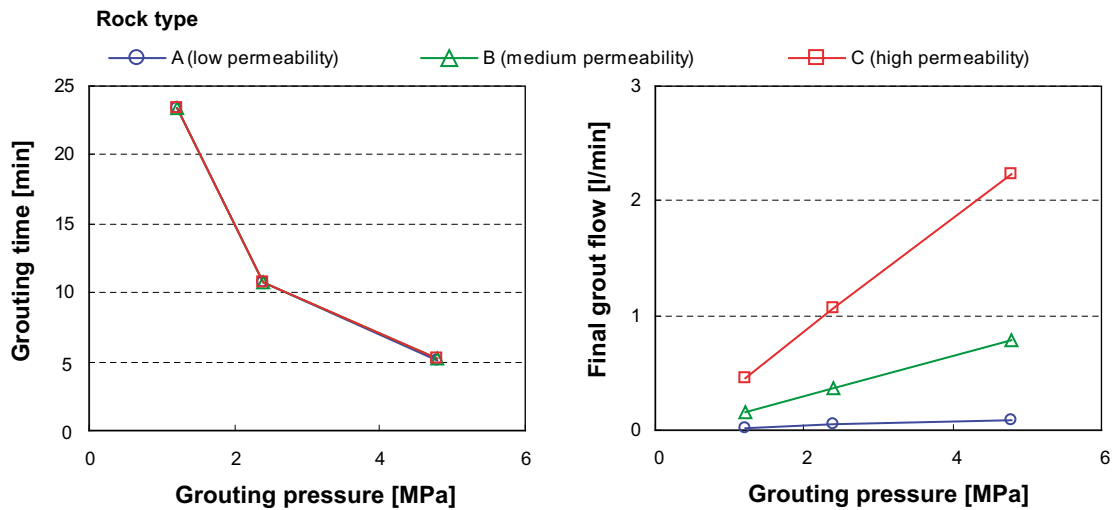
Figure 5-2. *Relationship between grouting pressure and calculated results for 1D case. The graph on the left shows calculated grouting time, while the graph on the right shows calculated final grouting flow.*

Figure 5-3. *Relationship between grouting pressure and calculated results for 2D case. The graph on the left shows calculated grouting time, while the graph on the right shows calculated final grouting flow.*

5.3.3   Effect of variation in yield strength

Figure 5-4 and Figure 5-5 show the relationship between the yield strength of the grout and the calculated results for the 1D and 2D cases, respectively.

In this parameter study, for the 1D case, the calculated grouting time and the final grout flow are not greatly influenced by yield strength. There is no difference between the calculated grouting times derived from different rock types, but high permeability results in high final grout flow.

The same can be said for the 2D case, with the exception of rock type C. This difference is also dependent on the capacity of the grouting equipment.

Figure 5-4. *Relationship between yield strength and calculated results for 1D case. The graph on the left shows calculated grouting time, while the graph on the right shows calculated final grouting flow.*
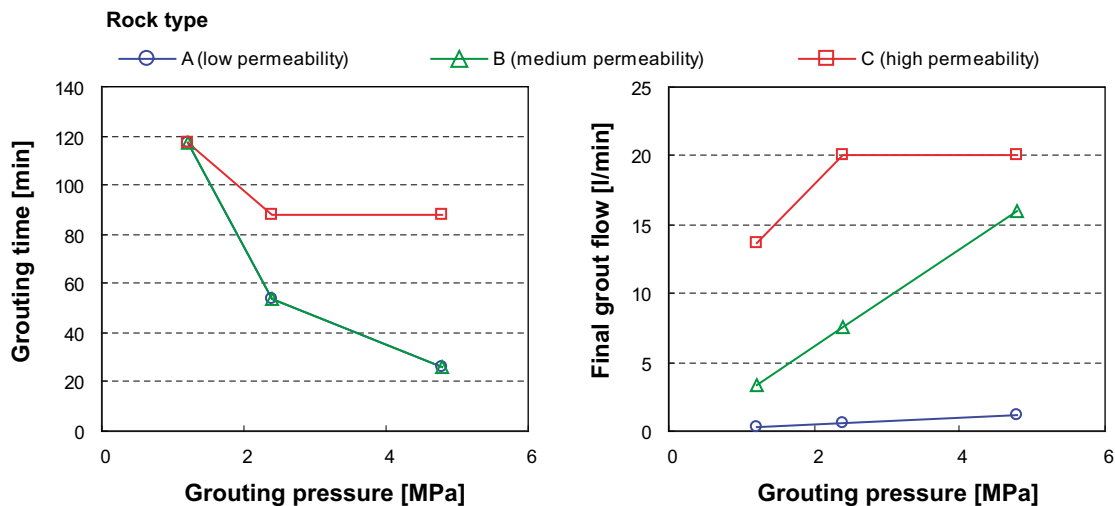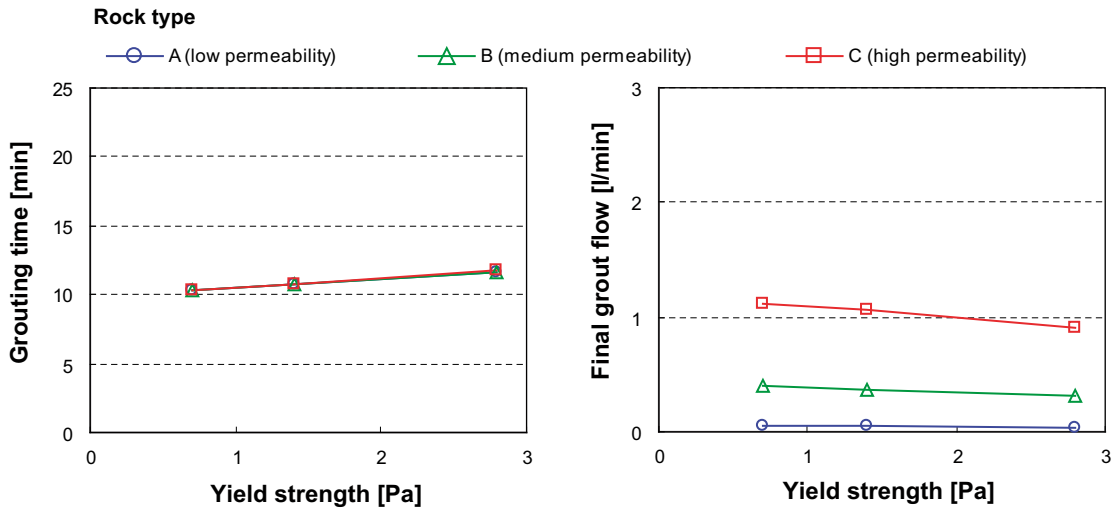

Figure 5-5. *Relationship between yield strength and calculated results for 2D case. The graph on the left shows calculated grouting time, while the graph on the right shows calculated final grouting flow.*

5.3.4 Effect of variation in viscosity

Figure 5-6 and Figure 5-7 show the relationship between viscosity of the grout and calculated results for the 1D and 2D cases, respectively.

For the 1D case, the calculated grouting time is proportional to the grouting pressure and there is no difference between the calculated grouting times derived from different rock types. However, the calculated final grout flow is inversely proportional to the grouting pressure, and high permeability results in high final grout flow.

The same can be said for the 2D case with the exception of rock type C. This difference is due to the capacity of the grouting equipment. Since the grout flow is limited to the capacity, the calculated grouting time is longer. The grouting time and the final grouting flow are dependent on the capacity of the grouting equipment in highly permeable rock.

Figure 5-6. *Relationship between viscosity and calculated results for 1D case. The graph on the left shows calculated grouting time, while the graph on the right shows calculated final grouting flow.*
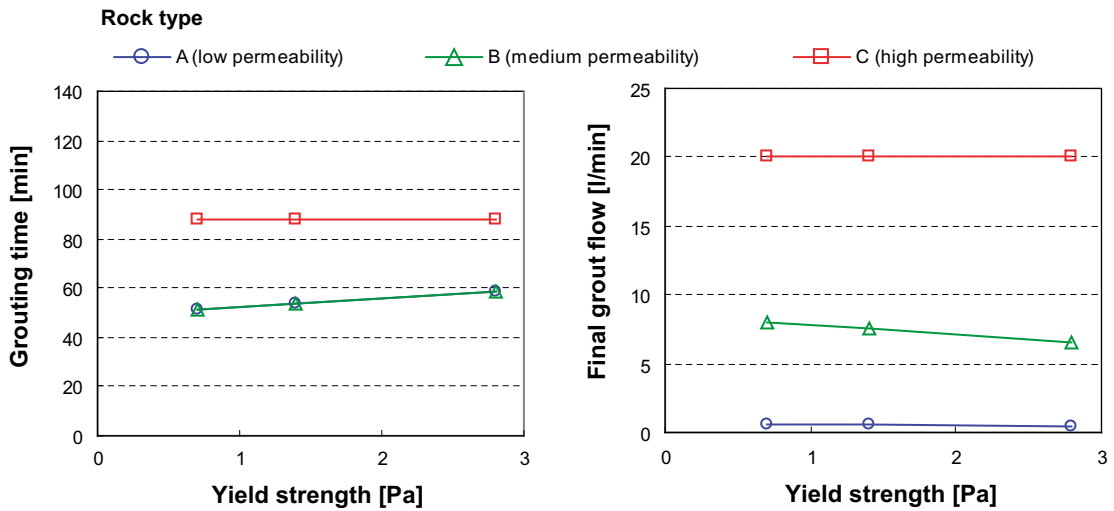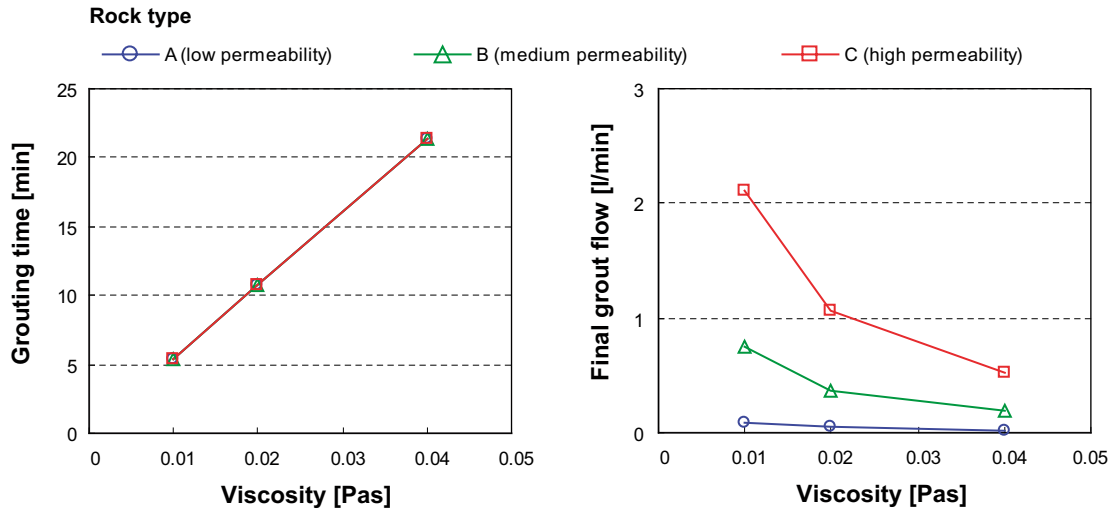

Figure 5-7. *Relationship between viscosity and calculated results for 2D case. The graph on the left shows calculated grouting time, while the graph on the right shows calculated final grouting flow.*
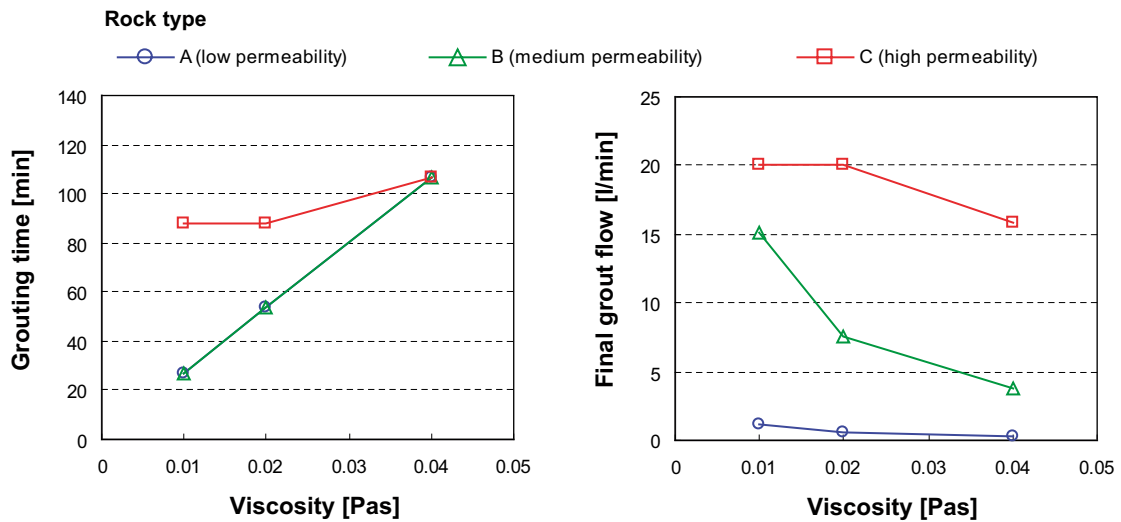
5.4 Conclusions

The effects of variations in grouting pressure, yield strength of the grout and viscosity of the grout were evaluated by calculating the grouting results with stop criteria based on grout penetration. The calculations were based on the further developed theory for both the 1D and 2D flows. Three types of hypothetical rock masses with different permeabilities are used for the calculations. The calculated results used for the comparison are grouting time and final grout flow, as the calculated grouted volume, which is dependent only on rock type and grout penetration, is the same for different grouting parameters.

The conclusion of the parameter analysis can be summarized as follows:

- The calculated grouting time is inversely proportional to the grouting pressure, and there is no difference between calculated grouting times derived from different rock types if the capacity of the grouting equipment is higher than the theoretical grout flow.

- High permeability results in high final grout flow for different grouting pressures. The calculated final grout flow is proportional to the grouting pressure if the capacity of the grouting equipment is higher than the theoretical grout flow.

- The calculated grouting time and the final grout flow are not influenced much by the yield strength of the grout in this parameter study. There is no difference between calculated grouting times derived from different rock types if the capacity of the grouting equipment is higher than the theoretical grout flow. High permeability results in high final grout flow for different yield strengths.

- The calculated grouting time is proportional to the viscosity of the grout and there is no difference between calculated grouting times derived from different rock types if the capacity of the grouting equipment is higher than the theoretical grout flow.

- High permeability results in high final grout flow for different viscosities of the grout. The calculated final grout flow is inversely proportional to the viscosity if the capacity of the grouting equipment is higher than the theoretical grout flow.

- The grouting time and the final grouting flow are dependent on the capacity of the grouting equipment in highly permeable rock because the capacity of the grouting equipment may be lower than the theoretical grout flow. Since the grout flow is limited to the capacity, the calculated grouting time is longer.

- The parameter study shows the effect of variation in grouting parameters. Although the grouting strategy is composed of many different components and the selection of a grouting method is complex, the theoretical design can be helpful in choosing an effective grouting method.

6 Conclusions and suggestions

6.1 Conclusions

The grouting theory concerning the relationship between grout penetration and grouting time has been developed in this report. The theory focuses on deriving theoretically based stop criteria for real grouting work. Then the developed theory has been verified by application to the field data from the grouting experiment at the 450 m level in the Äspö HRL. The theory has been used to analyze the difference between the grouting result based on theoretically based stop criteria and that based on the empirically based stop criteria, and the effects of variations in grouting parameters such as grouting pressure and grout materials have been evaluated.

The further developed grouting theory includes models for increasing the grouting pressure and changing the grout mix and the capacity of grouting equipments. Unlike in the case of increasing grouting pressure, extending the theory to include changing grout mixes is not a straightforward matter. Some manipulations are necessary in order to obtain the approximation. The lower and the upper boundaries of the theoretical solution for penetration length after changing the grout mix were therefore obtained. The lower boundary was calculated on the assumption that the properties of the pre-injected grout are the same as those of new grout and the upper boundary was calculated on the assumption that the properties of the pre-injected grout are the same as those of the groundwater. The capacity of the grouting equipment, such as a grout pump and a grout mixer, was taken into account as the maximum grouting flow and the maximum grouting pressure.

In order to verify the further developed theory, a comparison was made between the calculated result and the measured result by using the field data from the grouting experiment at the 450 m level in the Äspö HRL. Hydraulic apertures based on inflow and hydraulic apertures based on water loss measurements were both used for the calculation. It was concluded that the further developed theory is well verified and is applicable to grouting design and analysis, even though there is still room for further improvement.

In general the calculated results based on water loss measurement were better at predicting the actual results than those based on inflow. However, in one certain case the calculated grouting time based on inflow was closer to the measured result than that based on water loss measurement. This would indicate the importance of a deeper understanding of hydraulic aperture and an adequate fracture interpretation.

As for the penetration lengths after changes in grout mixes, the lower and the upper boundaries of the theoretical solution were calculated. When the grouted volume of the first grout was high, there was a big difference between the upper and the lower boundaries of the grouting result based on water loss measurement. The upper boundary was much higher than the measured result, but the lower boundary was close to the measured result. It can be said that the assumption for calculating the upper boundary that the pre-injected grout is the same as groundwater was unrealistic for this case and the assumption for calculating the lower boundary that the properties of the first grout are same as those of the second grout was close to the actual grouting situation. In order to evaluate the effect of changing grout mixes more accurately, a better approximation of the solution for changing grout mixes should be developed.

The difference between the grouting results based on three types of stop criteria – one based on grout flow, one on grout take, and the third on grout penetration – was analyzed using the theory. The calculations were done for both 1D and 2D flows. Three types of hypothetical rock masses with different permeabilities were used for the calculations. The big differences were found between all the results derived from three stop criteria for both the 1D and 2D cases.

In general, grouted volume and grouting time for the 2D case were much higher than those for the 1D case. The results show the importance of choosing the theoretically based stop criteria based on the estimated flow dimension of the fracture system in order to avoid inadequate or uneconomical grouting.

According to the calculation using the theory, it was found that the grout penetration is proportional to the fracture aperture, and that the grouting design with two grouting rounds is one solution to prevent excessive spreading of the grout for wider apertures in highly permeable rock types. The theoretical design based on grout penetration is very useful for choosing a good grouting design. Furthermore, the further developed theory is widely applicable to various grouting methods and makes it easy to calculate the grouting results.

The effects of variations in grouting pressure, yield strength of the grout and viscosity of the grout were evaluated by calculating the grouting results with stop criteria based on grout penetration. The calculations were based on the further developed theory for both 1D and 2D flows. Three types of hypothetical rock masses with different permeabilities were used for the calculations. It was found that the grouting time and the final grouting flow depend on the capacity of the grouting equipment in highly permeable rock because the capacity of the grouting equipment may be lower than the theoretical grout flow.

It was found in this case that the calculated grouting time is inversely proportional to the grouting pressure and there is no difference between the calculated grouting times derived from different rock types, and that the calculated final grout flow is proportional to the grouting pressure if the capacity of the grouting equipment is higher than the theoretical grout flow. High permeability results in high final grout flow for different grouting pressures.

It was found in this case that the calculated grouting time and the final grout flow are not much influenced by the yield strength of the grout, and that there is no difference between calculated grouting times derived from different rock types if the capacity of the grouting equipment is higher than the theoretical grout flow. High permeability results in high final grout flow for different yield strengths.

It was found in this case that the calculated grouting time is proportional to the viscosity of the grout and there is no difference between the calculated grouting times derived from different rock types, and that the calculated final grout flow is inversely proportional to the viscosity if the capacity of the grouting equipment is higher than the theoretical grout flow. High permeability results in high final grout flow for different viscosities of the grout.

The parameter study shows the effects of variations in grouting parameters. The grouting strategy is composed of many different components and the selection of a grouting method is complex. Therefore, the theoretical design can be helpful in choosing an effective grouting method.

6.2   Suggestions

In this report, several suggestions were presented for future research.

The important aspect of the theory that needs work is an approximation of the solution for changing grout mixes. There is no practical problem if the grouted volume of the first grout is low because there is little difference between the upper and the lower boundaries of the grouting result when the grout mix is changed. However, if this is not the case, the difference is great. In order to evaluate the effect of changing grout mixes more accurately, the theory for changing of grout mixes should be developed.

There are several ways to describe the geometry of a fracture, and it is not easy to choose a suitable hydraulic aperture for predicting and analyzing the grouting result. In the verification of the theory using the Äspö HRL data, the calculated results from hydraulic apertures based on

water loss measurement were generally better at predicting the actual results than those based on inflow during drilling. However, in one certain case the calculated grouting time based on inflow was closer to the measured result than that based on water loss measurement. A deeper understanding of the description of the fracture geometry is needed.

The theory is based on the assumption that every fracture has a constant aperture. However, in reality the fracture will have varying apertures and porosities in reality. The geometry of the fracture is more complicated. It is impractical to obtain the analytical solution by using all the information about fractures, but the theory should be improved to take account of more geological information such as porosities.

The calculation can be done for both the 1D and 2D cases, but the difference in calculated grouting result between the 1D and 2D cases was great. Estimating the flow dimension of the fracture system should be important. Furthermore, the grout flow could be between 1D and 2D, or more than 2D. The flow dimension of the fracture system should be taken into account to improve the theory.

In this report, the theory was verified by comparison of the calculated results with the measured results of the grouting experiment at the 450 m level in the Äspö HRL. The experiment was done under special conditions: a relatively tight crystalline rock mass at great depth. Further verification should be done using grouting data from other tunnels.

The grouting results used for comparison in order to verify the theory were grouted volume and grouting time. Grout penetration can be calculated by applying the theory, but this parameter is not visible in normal grouting work. In order to confirm the theory, a field test should be carried out to measure the penetration length directly.

It may be difficult to carry out grouting exactly as planned due to uncertain geological information, varying grouts, inaccurate grouting equipment, poor workmanship, and so on. In addition, knowing the parameters precisely beforehand is impossible because there are uncertainties inherent in the rock mass. The goal of future research is further development of the theory not only for determining the best grouting design in advance, but also for grouting management based on the actual rock mass at the construction site. The further study suggested above could make this possible.

References

Dalmalm T, 2004. Choice of grouting method for jointed hard rock based on sealing time predictions. PhD Thesis, Division of Soil and Rock Mechanics, Royal Institute of Technology, Stockholm.

Emmelin A, Eriksson M, Fransson Å, 2004. Characterisation, design and execution of two grouting fans at 450 m level, Äspö HRL. SKB R-04-58, Svensk Kärnbränslehantering AB.

Eriksson M, 2002. Prediction of grout spread and sealing effect. A probabilistic approach. PhD Thesis, Division of Soil and Rock Mechanics, Royal Institute of Technology, Stockholm.

Fransson Å, 2001. Characterisation of fractured rock for grouting using hydrogeological methods. PhD Thesis, Department of Geology, Chalmers University of Technology, Göteborg.

Gustafson G, Stille H, 1996. Prediction of groutability from grout properties and hydro geological data, Tunnelling and Underground Space Technology 11(3), pp 325–332.

Gustafson G, Claesson J, 2005. Steering Parameters for Rock Grouting, Submitted to Journal of Rock Mechanics and Mining Science.

Gustafson G, Stille H, 2005. Stop criteria for cement grouting, Felsbau 23(3), pp 62–68.

Gustafson G, Fransson Å, 2006. The use of the Pareto distribution for fracture transmissivity assessment, Hydrogeology Journal, 14(1–2), pp 15–20.

Håkansson U, 1993. Rheology of fresh cement-based grouts. PhD Thesis, Division of Soil and Rock Mechanics, Royal Institute of Technology, Stockholm.

Hässler L, 1991. Grouting of rock – Simulation and classification. PhD Thesis, Division of Soil and Rock Mechanics, Royal Institute of Technology, Stockholm.

Zimmerman RW, Bodvardsson GS, 1996. Hydraulic conductivity of rock fractures. Transport in Porous Media, Vol. 23, pp 1–30.

Inflow during drilling and estimated hydraulic apertures

Table A-1. Inflow during drilling, Fan 1:1.

Borehole/ Section	Inflow [l/min]					
	0–4.6m	4.6–7.6m	7.6–10.6m	10.6–13.6m	13.6–15.6m	Qtot
H4	0	0	0	3	42	45
C3	0	0	28	23	0	51
A2	0	1	0	119	12	132
A1	0	0	1	8	3	12
I5	0	0	132	0	0	132
G11	0	0	48	0	12	60
G10	0	0	24	0	72	96
D6	0	0	0	0	84	84
B7	0	0	12	10	122	144
B8	0	0	0	36	108	144
G9	0	0	5	5	44	54

Table A-2. Estimated hydraulic apertures based on inflow, Fan 1:1.

Borehole/ Section	Estimated hydraulic aperture [µm]				
	0–4.6m	4.6–7.6m	7.6–10.6m	10.6–13.6m	13.6–15.6m
H4	0	0	0	61	148
C3	0	0	129	121	0
A2	0	43	0	210	98
A1	0	0	45	84	61
I5	0	0	217	0	0
G11	0	0	155	0	98
G10	0	0	123	0	177
D6	0	0	0	0	187
B7	0	0	98	92	211
B8	0	0	0	141	203
G9	0	0	73	73	150

Table A-3. Inflow during drilling, Fan 1:2.

Borehole/ Section	Inflow [l/min] 0–4.6m	4.6–7.6m	7.6–10.6m	10.6–13.6m	13.6–15.6m	Qtot
I19	0	0	0	1.5	0.9	2.4
C15	0	0	0	24	0	24
I20	0	0	0	0	0.3	0.3
C16	0	0	0	21.6	0	21.6
D21	0	0	1	0	1.8	2.8
A14	0	0	0	0	0.1	0.1
D22	0	0	0	1	0	1
H17	0	0	0	2.4	0	2.4
B23	0	0	0.48	0	0.7	1.2
A13	0	0	1	6	2	9
B24	0	1	0	0	8	9
H18	0	0	0	1.3	1.7	3
B25	0	0	0	3	1.2	4.2
A12	0	0	0	0	1.8	1.8
G26	0	0	0	1	2	3
G31	0	0	0	0	0	0
G30						7.8
G29						0
G27						7.2
G28						7.2

Table A-4. Estimated hydraulic apertures based on inflow, Fan 1:2.

Borehole/ Section	Estimated hydraulic aperture [μm] 0–4.6m	4.6–7.6m	7.6–10.6m	10.6–13.6m	13.6–15.6m
I19	0	0	0	49	41
C15	0	0	0	123	0
I20	0	0	0	0	29
C16	0	0	0	119	0
D21	0	0	43	0	52
A14	0	0	0	0	21
D22	0	0	0	43	0
H17	0	0	0	57	0
B23	0	0	33	0	38
A13	0	0	43	77	54
B24	0	43	0	0	85
H18	0	0	0	46	51
B25	0	0	0	61	45
A12	0	0	0	0	52
G26	0	0	0	43	54
G31	0	0	0	0	0

Table A-5. Inflow during drilling, Fan 2:1.

Borehole/ Section	Inflow [l/min]						
	0–4.6m	4.6–7.6m	7.6–10.6m	10.6–13.6m	13.6–16.6m	16.6–18m	Qtot
G18	0	0	15	0	0	0	15
G19	0	0	9.9	0	0	0	9.9
G20	0	0	0	0	6.6	6.2	12.8
G17	0	0	2	0	4	12.6	18.6
A1	0	0	0	0	0	0	0
G16	0	0	4	0	0	32	36
A2	0	0	0	0	0	2.4	2.4
G15	0	0	3	0	6.6	27.6	37.2
A3	0	0	0	0	12.6	0	12.6
B14	0	0.5	0	0.5	0	2.6	3.6
A4	0	0	0	0.5	2.5	2.2	5.2
B13	0.5	0	0	0.5	0	2.6	3.6
C5	0	1.5	0	3.3	31.2	0	36
D10	0	0	0.5	3.4	0	0	3.9
B12	0	1	0	0	0	6.2	7.2
H6	0	0	0	0	22.8	0	22.8
D11	0.5	0	0.5	0	0	1.3	2.25
H7	0	0.5	0	0	19.9	0	20.4
I8	0	0	0.5	0	0	1.8	2.3
I9	0	3.6	0.6	0	0	0	4.2
I21	0	0	0	0	0	36	36

Table A-6. Estimated hydraulic apertures based on inflow, Fan 2:1.

Borehole/ Section	Estimated hydraulic aperture [µm]					
	0–4.6m	4.6–7.6m	7.6–10.6m	10.6–13.6m	13.6–16.6m	16.6–18m
G18	0	0	105	0	0	0
G19	0	0	91	0	0	0
G20	0	0	0	0	80	78
G17	0	0	54	0	68	99
A1	0	0	0	0	0	0
G16	0	0	68	0	0	135
A2	0	0	0	0	0	57
G15	0	0	61	0	80	129
A3	0	0	0	0	99	0
B14	0	34	0	34	0	59
A4	0	0	0	34	58	55
B13	34	0	0	34	0	59
C5	0	49	0	63	134	0
D10	0	0	34	64	0	0
B12	0	43	0	0	0	78
H6	0	0	0	0	121	0
D11	34	0	34	0	0	46
H7	0	34	0	0	115	0
I8	0	0	34	0	0	51
I9	0	65	36	0	0	0
I21	0	0	0	0	0	141

Water loss measurements

Table B-1. Water loss measurements in Fan 1:1.

Borehole no	Inflow natural (l)	Borehole length (m)	Waterloss length (m)	Time (min)	Final pressure (MPa)	Volume (l)	Flow, V/t (l/min)	Lugeon value
A1	7.2	15.6	15	1	0.5	11	11	1.5
A2	132	15.6	15	1	0.2	35	35	11.7
C3	45	15.6	15	1	0.15	28	28	12.5
H4	45	15.6	15	1	0.2	29	29	9.7
I5	132	15.6	15	1	0.15	45	45	20
D6	84	15.6	15	1	0.4	56	56	9.3
B7	144	15.6	15	1	0.2	52	52	17.3
B8	144	15.6	15	1	0.35	56	56	10.7
G9	60	15.6	15	1	0.65	40	40	4.1
G10	96	15.6	15	1	0.5	44	44	5.9
G11	60	15.6	15	1	0.65	42	42	4.3

Grouting data

Table C-1. Grouting data in Fan 1:1.

Hole number	Grouted volume [l]	Grouting time [min]
A1	154	41
A2	113	5
C3	198	26
H4	189	14
I5	184	5
D6	156	28
B7	177	8
B8	180	5
G9	115	31
G10	115	17
G11	53	17
Total	1,634	197

Table C-2. Grouting data in Fan 1:2.

Hole number	Grouted volume [l]	Grouting time [min]
A12	124	67
A13	140	49
A14	51	9
C15	224	56
C16	191	51
H17	129	43
H18	136	71
I19	78	35
I20	47	2
D21	87	39
D22	45	24
B23	77	38
B24	137	35
B25	232	59
G26	149	71
G27	178	52
G28	161	45
G29	54	7
G30	220	66
G31	77	35
Total	2,537	854

Table C-3. Grouting data in Fan 2:1.

Hole number	Grouted volume [l]	Grouting time [min]
A1	50	5
A2	61	6
A3	192	38
C4	169	43
C5	173	19
H6	203	17
H7	196	19
I8	35	20
I9	49	12
D10	13	6
D11	22	16
B12	133	45
B13	78	5
B14	42	18
G15	164	24
G16	156	23
G17	171	55
G18	153	37
G19	127	34
G20	107	18
I21	162	20
Total	2,456	480

Estimated hydraulic apertures based on water loss measurements

Table D-1. Estimated hydraulic apertures based on water loss measurements, Fan 1:1.

Borehole/ Section	Estimated hydraulic aperture [μm]				
	0–4.6m	4.6–7.6m	7.6–10.6m	10.6–13.6m	13.6–15.6m
H4	0	0	0	134	325
C3	0	0	296	278	0
A2	0	70	0	342	160
A1	0	0	82	154	112
I5	0	0	424	0	0
G11	0	0	236	0	149
G10	0	0	178	0	256
D6	0	0	0	0	329
B7	0	0	178	167	382
B8	0	0	0	217	312
G9	0	0	114	114	233

Calculated results from hydraulic apertures based on inflow

Table E-1. Calculated results from hydraulic apertures based on inflow in Fan 1:1.

Hole number	Lower boundary Grouted volume [l]	Grouting time [min]	Upper boundary Grouted volume [l]	Grouting time [min]
A1	0	0	0	0
A2	80	28	80	28
C3	48	45	48	45
H4	7	7	7	7
I5	80	28	80	28
D6	80	45	80	45
B7	80	25	80	25
B8	80	25	80	25
G9	77	70	77	70
G10	80	39	80	39
G11	80	64	80	64
Total	692	376	692	376

Table E-2. Calculated results from hydraulic apertures based on inflow in Fan 1:2.

Hole number	Lower boundary Grouted volume [l]	Grouting time [min]	Upper boundary Grouted volume [l]	Grouting time [min]
A12	0	0	0	0
A13	30	24	30	24
A14	0	0	0	0
C15	55	33	80	56
C16	30	10	35	15
H17	0	0	0	0
H18	0	0	0	0
I19	0	0	0	0
I20	0	0	0	0
D21	0	0	0	0
D22	0	0	0	0
B23	0	0	0	0
B24	30	24	30	24
B25	0	0	0	0
G26	0	0	0	0
G27	29	29	29	29
G28	29	29	29	29
G29	0	0	0	0
G30	30	28	30	28
G31	0	0	0	0
Total	233	175	263	203

Table E-3. Calculated results from hydraulic apertures based on inflow in Fan 2:1.

Hole number	Lower boundary Grouted volume [l]	Grouting time [min]	Upper boundary Grouted volume [l]	Grouting time [min]
A1	0	0	0	0
A2	30	90	30	90
A3	80	120	80	111
C4	30	81	30	81
C5	30	46	37	80
H6	80	38	90	79
H7	80	62	80	59
I8	80	73	80	69
I9	30	126	30	126
D10	30	60	30	60
D11	30	63	30	63
B12	0	0	0	0
B13	80	228	80	204
B14	30	81	30	81
G15	80	37	92	83
G16	80	38	90	79
G17	80	77	80	73
G18	80	98	80	92
G19	80	159	80	146
G20	80	117	80	109
I21	80	38	90	80
Total	1,170	1,632	1,219	1,767

Calculated results from hydraulic apertures based on water loss measurements

Table F-1. Calculated results from hydraulic apertures based on water loss measurements in Fan 1:1.

Hole number	Lower boundary Grouted volume [l]	Grouting time [min]	Upper boundary Grouted volume [l]	Grouting time [min]
A1	80	53	80	53
A2	95	20	130	33
C3	108	31	130	31
H4	80	7	130	42
I5	130	25	130	18
D6	80	8	130	44
B7	130	31	130	21
B8	80	7	130	37
G9	80	18	80	18
G10	80	12	88	20
G11	80	17	80	17
Total	1,023	229	1,238	334

Table F-2. Calculated results from 1.74 times as large as hydraulic apertures based on inflow in Fan 1:2.

Hole number	Lower boundary Grouted volume [l]	Grouting time [min]	Upper boundary Grouted volume [l]	Grouting time [min]
A12	30	22	30	22
A13	80	29	80	28
A14	0	0	0	0
C15	80	10	80	10
C16	80	11	80	11
H17	30	17	30	17
H18	30	13	30	13
I19	30	17	30	17
I20	0	0	0	0
D21	30	14	30	14
D22	0	0	0	0
B23	0	0	0	0
B24	80	29	80	28
B25	30	10	34	13
G26	30	13	30	13
G27	80	37	80	35
G28	80	37	80	35
G29	0	0	0	0
G30	80	34	80	33
G31	0	0	0	0
Total	770	292	774	290

Table F-3. Calculated results from 1.74 times as large as hydraulic apertures based on inflow in Fan 2:1.

Hole number	Lower boundary Grouted volume [l]	Grouting time [min]	Upper boundary Grouted volume [l]	Grouting time [min]
A1	0	0	0	0
A2	80	119	80	111
A3	80	20	130	178
C4	80	74	80	70
C5	82	60	82	58
H6	80	7	130	46
H7	80	11	130	79
I8	80	12	130	93
I9	80	129	80	120
D10	80	65	80	62
D11	80	70	80	66
B12	80	126	80	117
B13	80	36	92	85
B14	80	74	80	70
G15	80	7	130	44
G16	80	7	130	46
G17	80	13	130	103
G18	80	17	130	138
G19	80	26	109	130
G20	80	20	130	174
I21	80	7	130	46
Total	1,602	901	2,143	1,837

Calculated results of changed grouting design

Table G-1. Calculated results of changed grouting design from hydraulic apertures based on inflow in Fan 1:1.

Hole number	Lower boundary Grouted volume [l]	Grouting time [min]	Upper boundary Grouted volume [l]	Grouting time [min]
A1	0	0	0	0
A2	30	10	30	10
C3	30	27	30	27
H4	7	7	7	7
I5	30	10	30	10
D6	30	16	30	16
B7	30	9	30	9
B8	30	9	30	9
G9	30	26	30	26
G10	30	14	30	14
G11	30	23	30	23
Total	277	151	277	151

Table G-2. Calculated results of changed grouting design from hydraulic apertures based on water loss measurements in Fan 1:1.

Hole number	Lower boundary Grouted volume [l]	Grouting time [min]	Upper boundary Grouted volume [l]	Grouting time [min]
A1	30	19	30	19
A2	95	52	125	66
C3	108	60	130	66
H4	60	29	90	47
I5	130	40	130	35
D6	56	25	86	45
B7	130	49	130	42
B8	77	41	107	57
G9	30	6	30	6
G10	30	4	38	12
G11	30	6	30	6
Total	776	331	926	401